Several phased siRNA annotation methods can frequently misidentify 24 nucleotide siRNA-dominated *PHAS* loci

Seth Polydore[1,2], Alice Lunardon[2], and Michael J. Axtell[1,2*]

1. Genetics Ph.D. Program, Huck Institutes of the Life Sciences, The Pennsylvania State University, University Park, PA 16802 USA.
2. Department of Biology, The Pennsylvania State University, University Park, PA 16802 USA.

* Corresponding author: mja18@psu.edu

Abstract

Small RNAs regulate key physiological functions in land plants. Small RNAs can be divided into two categories: microRNAs (miRNAs) and short interfering RNAs (siRNAs); siRNAs are further sub-divided into transposon/repetitive region-localized heterochromatic siRNAs and phased siRNAs (phasiRNAs). PhasiRNAs are produced from the miRNA-mediated cleavage of a Pol II RNA transcript; the miRNA cleavage site provides a defined starting point from which phasiRNAs are produced in a distinctly phased pattern. 21-22 nucleotide (nt)-dominated phasiRNA-producing loci (*PHAS*) are well represented in all land plants to date. In contrast, 24 nt-dominated *PHAS* loci are known to be encoded only in monocots and are generally restricted to male reproductive tissues. Currently, only one miRNA (miR2275) is known to trigger the production of these 24 nt-dominated *PHAS* loci. In this study, we use stringent methodologies in order to examine whether or not 24 nt-dominated *PHAS* loci also exist in *Arabidopsis thaliana*. We find that highly expressed heterochromatic siRNAs were

consistently mis-identified as 24 nt-dominated *PHAS* loci using multiple *PHAS*-detecting algorithms. We also find that *MIR2275* is not found in *A. thaliana*, and it seems to have been lost in the last common ancestor of Brassicales. Altogether, our research highlights the potential issues with widely used *PHAS*-detecting algorithms which may lead to false positives when trying to annotate new *PHAS*, especially 24 nt-dominated loci.

Introduction

Small RNAs regulate key physiological functions in land plants, ranging from organogenesis (Boualem et al., 2008, 2008; Kutter et al., 2007; Laufs et al., 2004; Williams et al., 2005) to gametogenesis (Grant-Downton et al., 2009). Three major protein families are involved in the biogenesis of small RNAs. The first family is the DICER-LIKE (DCL) protein family. Consisting of four paralogs in the *Arabidopsis thaliana* genome (Baulcombe, 2004; Chapman & Carrington, 2007), DCL proteins hydrolyze RNA precursors into 20-24 nt double-stranded RNA fragments (Millar & Waterhouse, 2005). These double-stranded RNA fragments are then loaded into ARGONAUTE (AGO) proteins, the second protein family, and one strand of the RNA is discarded (Ender & Meister, 2010). Upon Watson-crick binding to other RNA transcripts in the cell, the AGO/single-stranded RNA complex represses other RNA transcripts (Baumberger & Baulcombe, 2005; Qi et al., 2005). Overall, 10 AGOs are encoded in the *A. thaliana* genome (Tolia & Joshua-Tor, 2007). RNA DEPENDENT RNA POLYMEREASES (RDRs) are the third family of proteins involved in the biogenesis of many small RNAs. RDRs convert single-stranded RNAs into double-stranded RNAs by synthesizing the complementary strand of the RNA molecule (Willmann, et al., 2011). Six *RDRs* are encoded in the *A. thaliana* genome (Willmann, et al., 2011).

Small RNAs can be divided into two major categories: microRNAs (miRNAs) which are precisely processed from single-stranded RNA with a hairpin-like secondary structure (Millar & Waterhouse, 2005), and short interfering RNAs (siRNAs), which are derived from double-stranded RNA precursors (Axtell, 2013). siRNAs are further divided into several different groups, including phased siRNAs (phasiRNAs) and heterochromatic siRNAs (hc-siRNAs). Predominantly 24 nts in length, hc-siRNAs function to repress transcription of deleterious genomic elements such as transposable elements or repetitive elements (Ahmed et al., 2011) and the promoters of certain genes (Baev et al., 2010) by reinforcing the presence of heterochromatin in targeted areas (Baulcombe, 2004; Sugiyama et al., 2005). Biogenesis of hc-siRNAs begins with transcription by the plant-specific, holo-enzyme DNA DEPENDENT RNA POLYMERASE IV (Pol IV) (Onodera et al., 2005). The resulting transcript is then converted into double-stranded RNA by RDR2 and this double-stranded transcript is hydrolyzed by DCL3 (Matzke et al., 2009). phasiRNAs are derived from DNA DEPENDENT RNA POLYMERASE II (Pol II) transcripts that have been targeted by miRNAs (Fei et al., 2013). Upon miRNA-mediated hydrolysis, the RNA transcript is converted into double-stranded RNA by RDR6 (Cuperus et al., 2010). The resulting double-stranded RNA is then cleaved into 21nt double-stranded RNA fragments by DCL4 (and less frequently DCL2) (Axtell et al., 2006).

21-22 nt phasiRNA-producing loci (*PHAS*) are clearly represented in all land plants that have been sequenced thus far (Fei et al., 2013; Zheng et al., 2015). However, 24 nt dominated *PHAS* loci are only currently described in rice (Song et al., 2011), maize (Zhai et al., 2015), and other non-grass monocots (Kakrana et al., 2018). Much like 21 nt-dominated *PHAS*, the biogenesis of these 24 nt-dominated *PHAS* loci begins with the Pol II-dependent transcription of a single-stranded RNA precursor which is then targeted by miR2275 and hydrolyzed. To date,

69 miR2275 is the only miRNA known to trigger the production of 24 nt-dominated phasiRNAs
70 (Fei et al., 2013). The resulting RNA transcript is then converted into a double-stranded RNA
71 molecule by RDR6 (Zhai et al., 2015). However, these phasiRNA precursors are then
72 hydrolyzed by DCL5 (a DCL3 homolog sometimes called DCL3b) to produce 24 nt phasiRNAs
73 (Fei et al., 2013).

74 Aside from the combination of their size and biogenesis patterns, 24 nt-dominated *PHAS*
75 loci are distinct in various ways. These loci as well as their triggering miRNA, miR2275, are
76 very specifically expressed in the tapetum during early meiosis and quickly recede in expression
77 in other stages of male gametogenesis in rice and maize (Tamim et al., 2018). The AGO protein
78 that loads these phasiRNAs is unknown; however, in maize, *AGO18b* expression levels match
79 those of the 24 nt-dominated *PHAS* loci quite closely and is therefore the most likely candidate
80 to load 24 nt phasiRNAs (Komiya et al., 2014; Zhang et al., 2015). The targets of these 24 nt
81 phasiRNAs are unknown, but they are apparently necessary for proper male gametogenesis (Ono
82 et al., 2018). 24 nt-dominated *PHAS* loci were also described in the non-grass monocots
83 asparagus, lily, and daylily (Kakrana et al., 2018). These phasiRNAs are produced from
84 processing of inverted repeat (IR) RNAs, instead of the double-stranded RNA precursors
85 observed in rice and maize (Kakrana et al., 2018). Although the 24 nt-dominated *PHAS* loci
86 from non-grass monocots are still expressed most greatly in male reproductive tissue, in
87 asparagus they are also expressed in female reproductive tissue (Kakrana et al., 2018).

88 We set out to search for evidence of 24 nt-*PHAS* loci in plants besides monocots. We
89 searched for 24 nt *PHAS* loci in the *A. thaliana* genome using small RNA-seq data. Currently,
90 several distinct algorithms are available to calculate the "phasing" of a sRNA-producing locus
91 (Dotto et al., 2014; Guo et al., 2015; Zheng et al., 2014). In general, these algorithms calculate

92 the number of reads that are "in-phase" against those that are "out-of-phase" in order to
93 determine the likelihood that a particular locus truly produces phasiRNAs (Axtell, 2010).
94 However, 24 nt-dominated siRNA loci are very numerous in angiosperms, and therefore are a
95 potential source of false-positives during searches for *PHAS* loci. We therefore carefully
96 examined *A. thaliana* 24 nt-dominated loci that consistently passed *PHAS*-locus detecting
97 algorithms using multiple methods find that they are likely just heterochromatic siRNAs (hc-
98 siRNAs). We also use two other methods to examine the presence of 24 nt-dominated *PHAS*
99 loci in the *A. thaliana* genome. We searched for *rdr6*-dependent, 24 nt-dominated loci and found
100 18 such loci. We also examined homology of the miR2275 which triggers 24 nt phasiRNA
101 biogenesis in rice and maize but found that the Brassicales clade contains no potential homologs
102 for this miRNA. Overall, our results suggest that there are no true 24 nt *PHAS* loci in *A.*
103 *thaliana*. Furthermore, our analysis shows that existing phasing score algorithms to detect novel
104 *PHAS* loci can lead to false positives.

105

106 **Results**

107 **miR2275 is not found in the *Brassicales* clade**

108 Currently known 24 nt dominated phasiRNA precursors are known to be targeted only by
109 a single miRNA family, miR2275 (Song et al., 2008; Zhai et al., 2015). We examined all
110 available angiosperm genomes on Phytozome (ver 12.1) for potential homologs of *MIR2275*. In
111 monocots, all but *Brachypodium stacei, Spirodela polyrhiza* and *Zostera marina* had potential
112 miR2275 homologs (Figure 1; Figure S1). 12 eudicots had potential miR2275 homologs based
113 on sequence similarity (Figure 1). We therefore interrogated small RNA libraries for these

114 species to see if a mature miR2275 homolog was expressed. Five eudicots had evidence of
115 mature miR2275 accumulation (Figure 1). All of the monocots for which we obtained small
116 RNA-seq data expressed mature miR2275, except *Musa acuminata* (Figure 1). Alignment of the
117 *MIR2275* loci in species for which potential homologs could be identified shows strong
118 conservation of the mature miRNA and miRNA* sequences (Figure S2), suggesting that these
119 loci evolved from a common ancestor. Importantly, because of the high specificity of miR2275
120 expression in developing anthers (Tamim et al., 2018), it's possible that our analysis includes
121 false negatives, especially in situations where no reproductive tissue small RNA libraries were
122 available. Altogether, our data suggest that miR2275 is not found in *A. thaliana* and that this
123 loss apparently occurred before the last common ancestor for Brassicales.

124

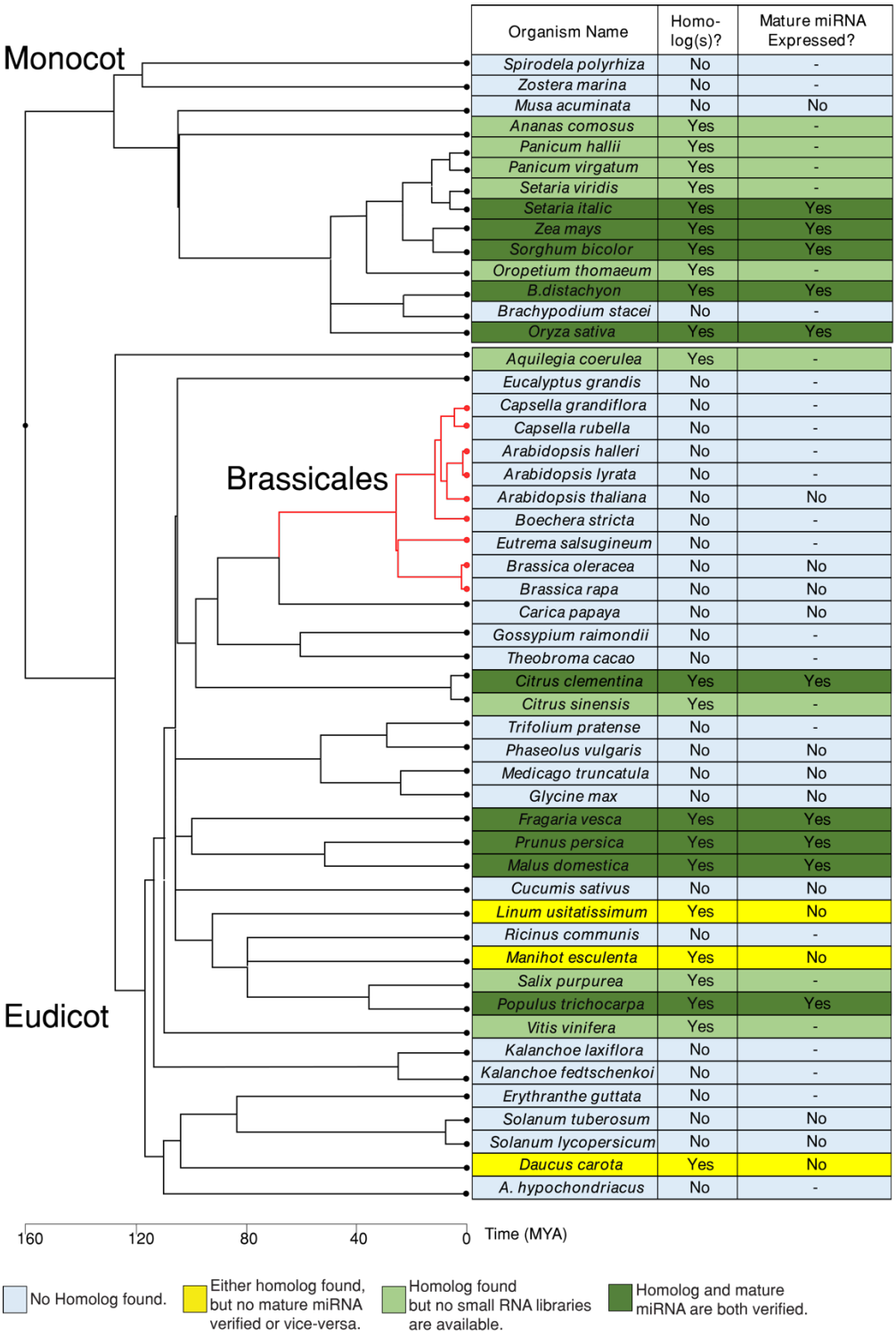

Figure 1. Conservation of *MIR2275*.

Evidence for existence of *MIR2275* homologs in angiosperms. Phylogeny depicts estimated divergence times per TimeTree of Life (Kumar et al., 2017).

Three *A. thaliana* hc-siRNA loci consistently pass *PHAS*-detecting algorithms

Although *A. thaliana* lacks miR2275, it's possible that 24 nt *PHAS* loci exist in *A. thaliana* and are triggered by a different small RNA. We reasoned that true 24 nt *PHAS* loci would be dependent on one or more of the well-described *A. thaliana RDR* genes: *RDR1, RDR2,* or *RDR6*. We thus examined a previously described differential expression analysis that identified *A. thaliana* small RNA loci that were down-regulated in an *rdr1/rdr2/rdr6* triple mutant (Polydore & Axtell, 2018). The phase scores of *rdr1/rdr2/rdr6*-dependent, 24 nt-dominated loci were calculated in eight independent small RNA libraries using three different algorithms (Figure 2a). Reasonable cut-offs for *PHAS* loci detection were determined by examining the phase score distributions in the three merged wild-type libraries when well-known 21 nt *PHAS* loci were analyzed (Figure S3). These cutoffs were consistent when a larger number of sRNA-seq libraries were examined (Figure S4). Of the 31,750 loci examined, only three (Figure S5; Dataset S1) passed the *PHAS* loci algorithms consistently in all 8 libraries examined (Figure 2a).

We were interested in determining why these three loci consistently pass the *PHAS*-detection algorithms. As phasiRNA precursors are known to be targeted by miRNAs, we predicted whether or not any known *A. thaliana* miRNAs could target these three loci. We were unable to find any obvious miRNA target sites at these loci. Although miRNA target sites were not apparent at these loci, it's entirely possible that other siRNAs might target them and initiate siRNA phasing. We therefore attempted to determine the most common phase register at each of these loci in the 8 different wild-type libraries (Figure S6). If these loci are truly phased, then we would expect the same phase register to predominate in each library examined. While this was the case for *TAS2* (a positive control), none of the three 24 nt loci passing the *PHAS*-detection

153 algorithms had consistent phase registers (Figure S6). We also note that these three loci didn't
154 have the majority of their mapped reads falling into a single phase register in any of the libraries
155 examined, as one would expect for a true *PHAS* locus (Figure S6).

156

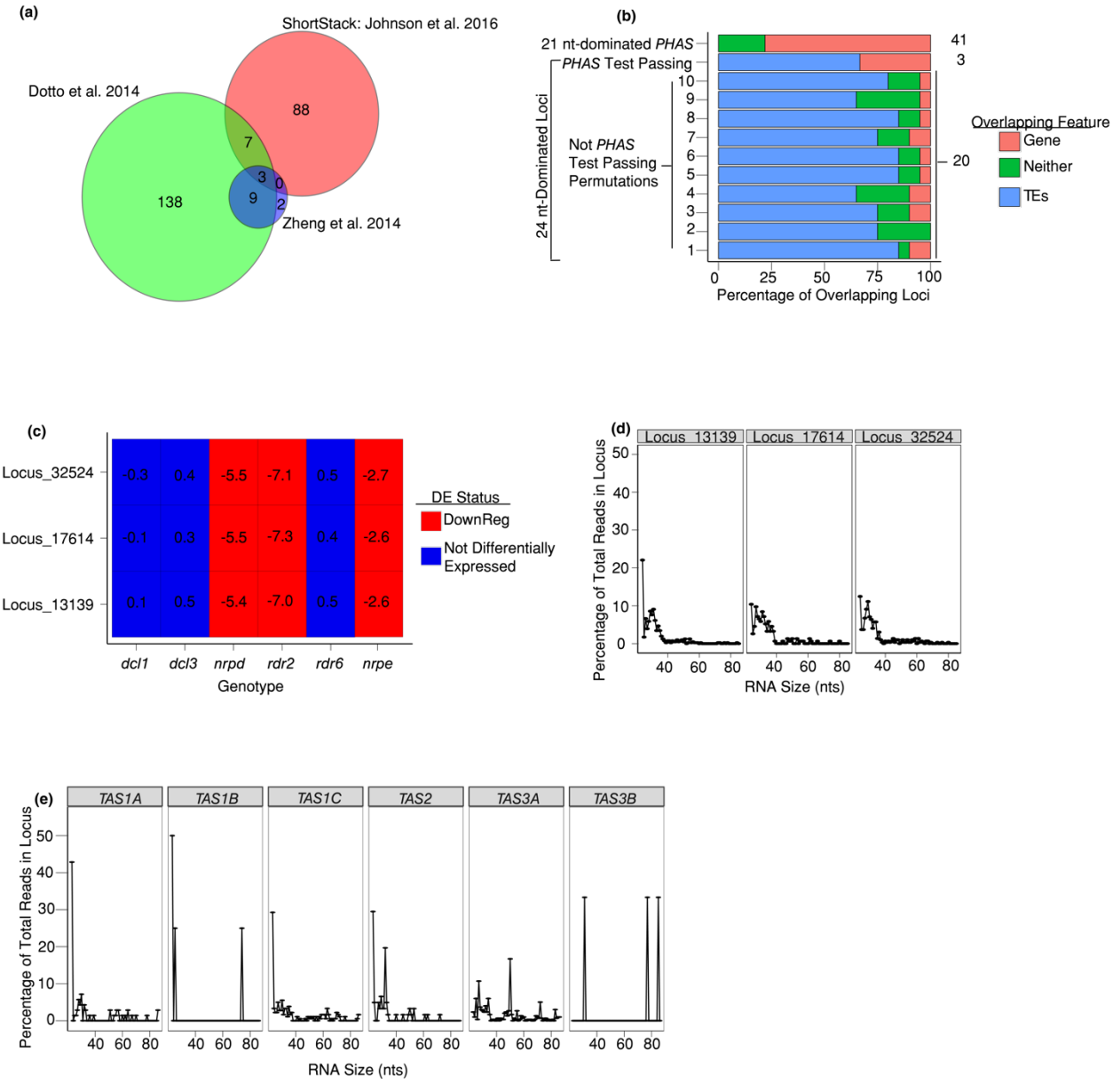

157

158

Figure 2. Properties of three *A. thaliana* 24 nt-dominated small RNA loci that were called 'phased' by three different methods.

(a) Venn diagram shows numbers of 24 nt-dominated loci that were called 'phased' by the indicated algorithms.

(b) Percentage of the three *PHAS*-test passing loci overlapping either genes or transposable elements. The percentage is calculated as: (number of loci intersecting a feature/total number of loci in category)*100. The total number of loci in each category is given on the right. For 24 nt not-*PHAS* loci, ten randomly selected cohorts of 20 loci each are shown.

(c) Accumulation of the three *PHAS*-test passing loci in different genetic backgrounds. Numbers represent the ratio of small RNA accumulation in the indicated genotypes over that in corresponding wild-type library as computed by DESeq2. The differential expression status was determined via DESeq2 at an FDR of 0.1.

(d) Percentage of short RNAs from *dcl2/dcl3/dcl4* triple mutant libraries by read length for the three *PHAS*-test passing loci.

(e) Same as in Panel d, except for five known *A. thaliana TAS* loci.

We then determined where in the genome these loci were encoded. Similar to hc-siRNA loci, these three loci primarily overlap with repeat- and transposable-elements (Figure 2b). In comparison, many known *A. thaliana PHAS* loci are primarily derived from genes (Figure 2b). Rice and maize annotated 24 nt *PHAS* loci are derived from long non-coding RNAs that are encoded in regions of the genome that are devoid of protein-coding genes, transposable elements, or repeats (Song et al., 2008; Zhai et al., 2015). We also note that sRNA accumulation from these three loci is down-regulated in *nrpd1-3* (NRPD is the largest sub-unit of Pol IV), *nrpe* (NRPE is the largest subunit of Pol V), and *rdr2* (Figure 2c). hc-siRNAs have the same genetic requirements (Matzke et al., 2009), which strongly suggests that these three loci produce hc-siRNAs. Notably, these loci are not down-regulated in *dcl3* backgrounds. This is in line with past data that show that DCL4 and DCL2 can partially complement production of hc-siRNAs in *dcl3* backgrounds (Gasciolli et al., 2005).

187 The Pol IV transcripts from which hc-siRNAs are derived are around 26-50 nts in length,
188 and accumulate to detectable levels in the *dcl2-1/3-1/4-2t* (*dcl234*) triple mutant (Ye et al., 2016;
189 Zhai et al., 2015). We therefore analyzed the lengths of reads mapping to our three putative 24
190 nt *PHAS* loci in *dcl234* triple mutants. We found most reads were less than 40 nts long,
191 indicating that these putative 24 nt *PHAS* loci are associated with short precursors similar to hc-
192 siRNA loci (Figure 2d). In comparison, reads mapping to the known *TAS* loci had a wider range
193 of sizes, ranging from 24-80 nts (Figure 2e). Overall, the size profile of the precursor RNAs
194 further delineate these three loci from known *PHAS* loci.

195 Finally, we examined the AGO-enrichments of small RNAs from these loci. Canonical
196 hc-siRNAs are loaded into AGO4 in order to repress other loci transcriptionally (Mi et al., 2008).
197 While sRNAs from our three putative 24 nt *PHAS* loci are not particularly enriched in AGO4-
198 immunoprecipitation libraries, known 21 nt *PHAS* loci are quite depleted in the same dataset
199 (Figure S7). We also note that sRNAs from the three putative 24 nt *PHAS* loci are depleted in
200 AGO1 immunoprecipitation libraries (Figure S7), probably owing to the lack of 21 nt sRNAs,
201 which AGO1 primarily loads, produced at these loci (Mi et al., 2008).

202

203 **The three *PHAS*-Test passing loci have distinct characteristics**

204 hc-siRNAs are known to produce small RNAs in a very imprecise manner, unlike the
205 largely precise processing of phasiRNAs (Axtell, 2013). We were interested in how three hc-
206 siRNAs could consistently pass three different *PHAS*-detecting algorithms. One simple
207 explanation is possible erroneous placement of ambiguously mapped reads. These multi-
208 mapping reads could cause the *PHAS*-detecting algorithms to overestimate the number of "in
209 phase" reads. We therefore determined the proportion of multi-mapping reads in each locus, but

these loci have low proportion of multi-mapping reads compared to other 24 nt-dominated loci (Figure 3a). We note that these three loci are more highly expressed than most other 24 nt-dominated loci and even known *PHAS* loci in *A. thaliana* (Figure 3b). These three loci accumulate to nearly 1,000 RPM, while most other 24 nt-dominated loci and known *PHAS* loci only produce around 1 RPM (Figure 3b). Another interesting feature of these loci is their length. All three of these loci are around 10,000 nts in length, far greater than the 200-800 nt length of canonical *PHAS* loci and most other 24 nt-dominated loci (Figure 3c). These results indicate that these loci are simply highly expressed and particularly long hc-siRNA producing loci (Figure S3).

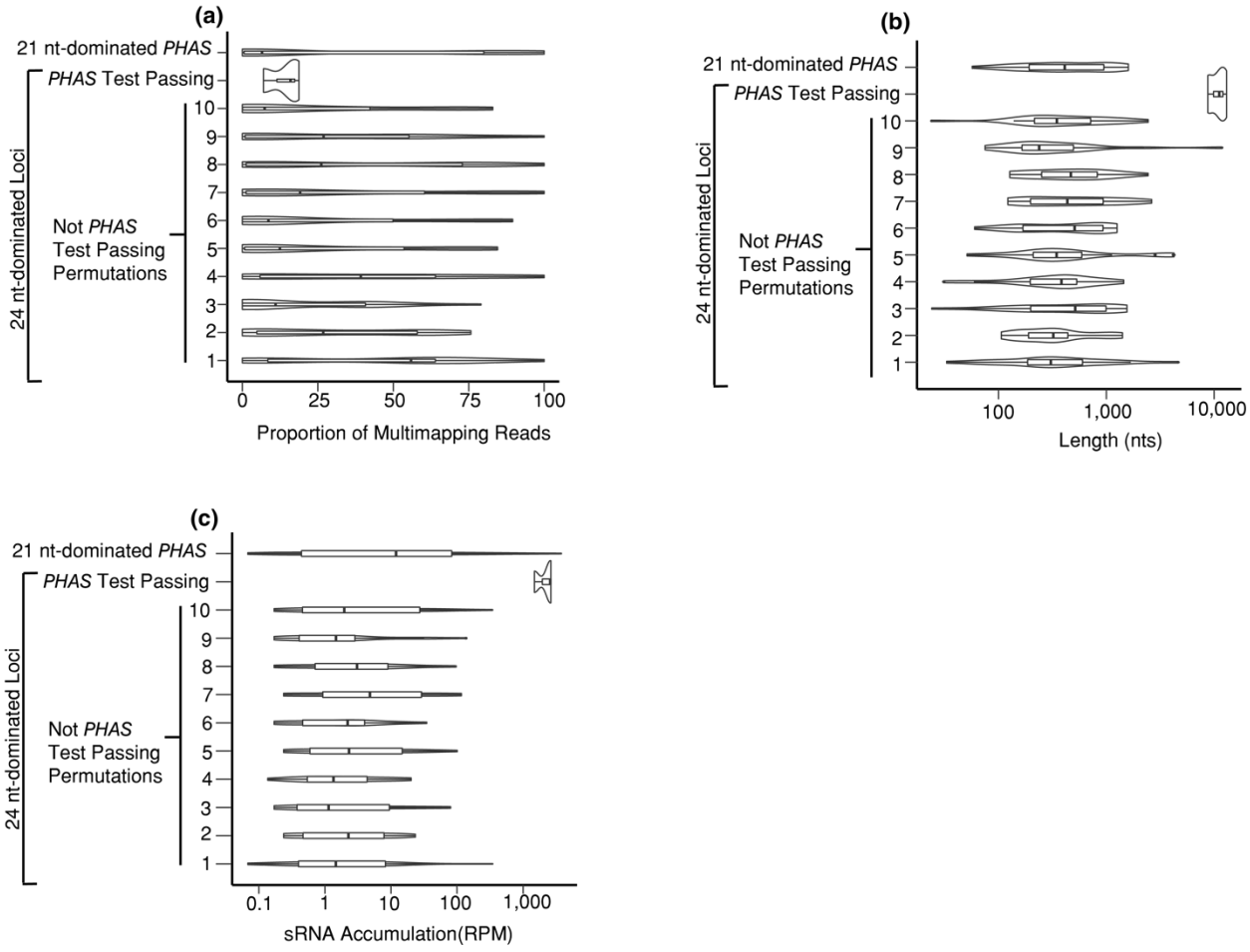

Figure 3. The three *PHAS*-Test passing small RNA loci have distinct properties compared to other 24 nt-dominated Loci.

(a) The proportion of multi-mapped reads in three different types of small RNA loci. For 24 nt-dominated loci that were not called PHAS loci, ten cohorts comprising 20 randomly selected loci were used as controls. The width of the density plot shows the frequency. The inset boxes show medians (horizontal lines), the 1st-3rd quartile range (boxes), the 95% confidence of medians (notches), other data out to 1.5 times the interquartile range (whiskers) and outliers (dots).

(b) Same as panel a except showing small RNA accumulation.

(c) Same as panel a except showing small RNA locus length.

A small number of *A. thaliana rdr6*-dependent, 24 nt-dominated siRNA loci exist, but are not phased

Canonical monocot 24 nt-dominated *PHAS* loci are produced in part through the biochemical activity of RDR6 (Zhai et al., 2015). We therefore used an alternative strategy to identify possible 24 nt *PHAS* loci by first identifying *rdr6*-dependent, 24 nt-dominated siRNA loci. We found 18 such loci (Figure S8; Dataset S1). None of these loci were consistently phased in the eight wild-type, inflorescence *A. thaliana* libraries (Table S2) tested according to any of the three algorithms we used (Dataset S3). We determined the genetic dependencies of these loci and found that these loci are down-regulated in *nrpd, nrpe,* and *rdr2* backgrounds (Figure 4). Furthermore, these loci either overlap transposable elements or are mostly found in otherwise intergenic regions (Figure S9a). As these are typical features of hc-siRNAs, it's possible that hc-siRNAs simply erroneously placed at these loci. Again, we examined the proportion of ambiguously mapped reads in these *rdr6*-dependent, 24 nt-dominated loci compared to other 24 nt-dominated loci and found that these loci had low proportions of multi-mapping reads (Figure S9b). Our result argues against this hypothesis.

247 *rdr6*-dependent, 24 nt-dominated loci are strongly expressed relative to other 24 nt-
248 dominated loci (Figure S9c). These *rdr6*-dependent loci have median expression level of nearly
249 100 RPM compared to the nearly 1 RPM median expression level of the other 24 nt-dominated
250 loci (Figure S9c). This result is similar to the three *A. thaliana* loci that passed our *PHAS*-
251 detection algorithms (Figure 3b). However, the lengths of the *rdr6*-dependent, 24 nt-dominated
252 loci are similar to other 24 nt-dominated loci (Figure S9d). Overall while do find evidence for a
253 small number of *rdr6*-dependent, 24 nt dominated siRNAs in *A. thaliana*, they are not phased,
254 nor do they appear readily discernable from more typical hc-siRNA loci. Thus we find no
255 evidence of 24 nt dominated *PHAS* loci in *A. thaliana*.

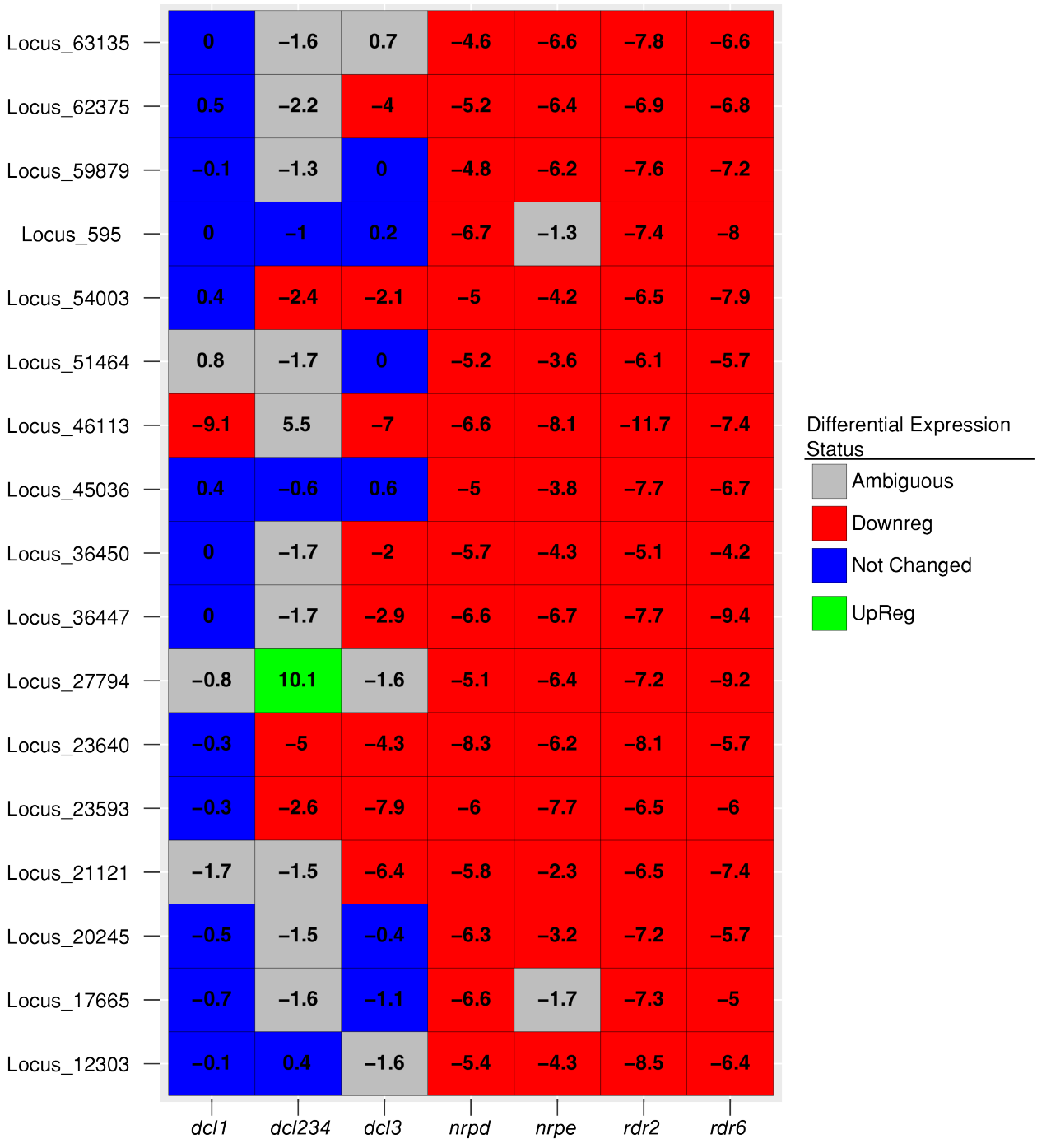

Figure 4. Accumulation of 24 nt-dominated, *rdr6*-dependent small RNA loci in different mutant backgrounds.

Numbers represent the log2-transformed ratios of small RNA accumulation in the indicated genotypes over that in corresponding wild-type library as computed by DESeq2. The differential expression status was determined via DESeq2 at an FDR of 0.1.

Erroneous detection of 24nt-domination *PHAS* loci occurs in other land plant species

We were interested in determining if erroneous annotation of *PHAS* loci was unique to *A. thaliana* small RNAs or if these results could be replicated in other species. We therefore interrogated publicly available *Brassica rapa*, *Cucumis sativus*, *Phaseolus vulgaris*, and *Solanum tuberosum* small RNA libraries (all eudicots) using the three algorithms, searching for putative 24 nt-dominated *PHAS* loci. We specifically chose these four species because they all lacked a potential *MIR2275* homolog (Figure 1). As miR2275 is the only miRNA known to trigger 24 nt-dominated phasiRNAs, any 24 nt-dominated loci called as *PHAS* loci in these species are likely false positives. Each species had 24 nt-dominated small RNAs that were misannotated as *PHAS* loci (Figure S10). We first determined where in the genome the 24 nt-dominated loci are encoded. Like in *A. thaliana,* 24 nt-dominated loci that passed the *PHAS*-detection algorithm seem to come predominantly from transposable elements. This was true in all the species examined except for *P. vulgaris* (Figure 5a). Curiously, the *PHAS*-test passing loci had a slightly higher proportion of ambiguously mapped reads compared to other 24 nt-dominated loci in *B. rapa*, *P. vulgaris*, and *S, tuberosum* (Figure 5b). For *C. sativus*, the proportion of multi-mapping reads in *PHAS*-test passing 24 nt-dominated loci was substantially higher than other 24 nt-dominated loci (Figure 5b). It's still unlikely that multi-mapping reads contribute significantly to phasing at these loci as the proportion of ambiguously mapped to both types of 24 nt-dominated loci are similar in three of the four species tested (Figure 5b).

In the four species tested, the *PHAS*-test passing 24 nt-dominated loci had both significantly greater lengths (Figure 5c) and expression on average (Figure 5d). We observed this same trend in *A. thaliana* (Figure 3b-c), which suggests that long lengths and high

285 expression levels of 24 nt-dominated loci are conducive to *PHAS* loci mis-annotations, even in

286 other distantly related species.

287

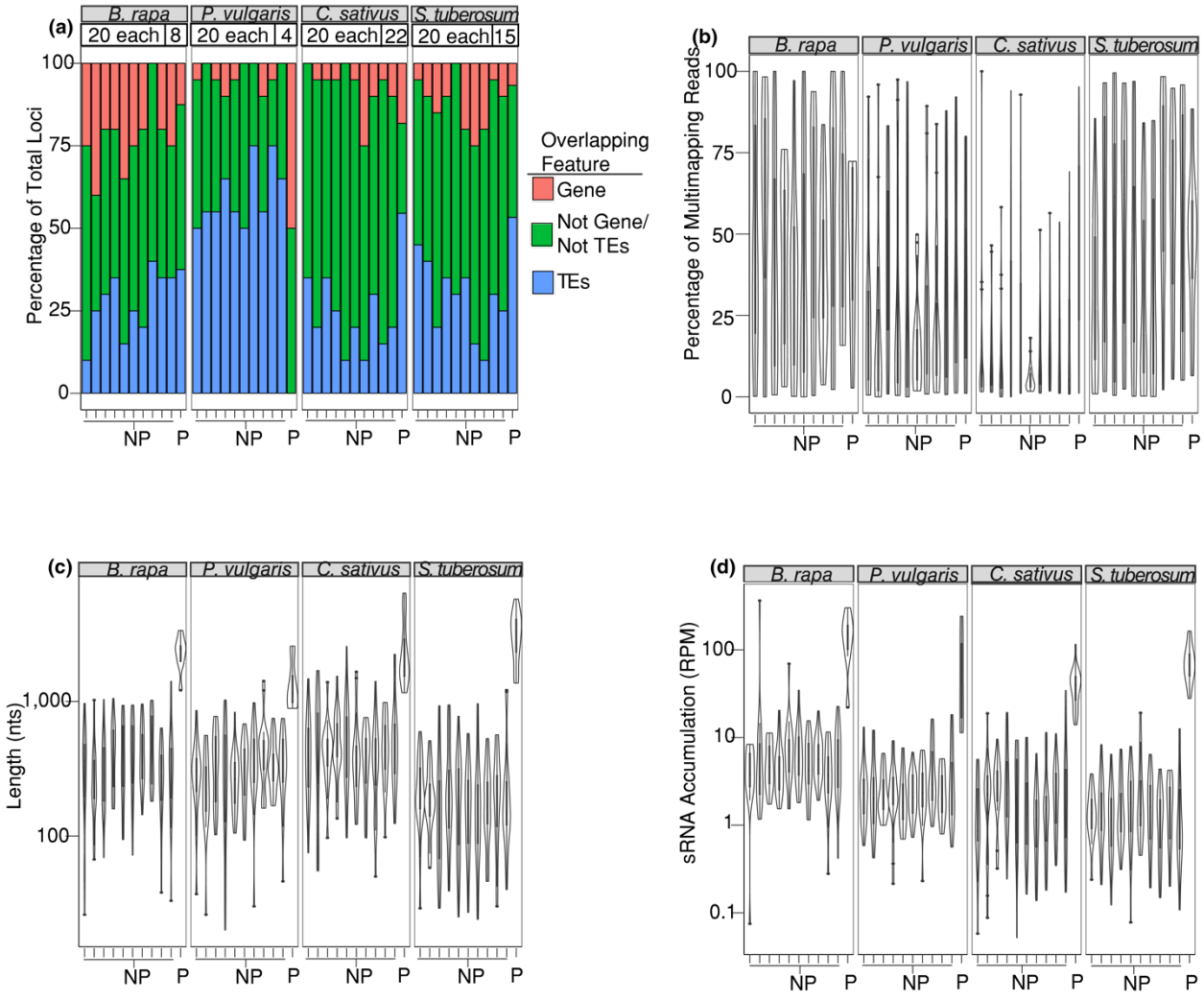

288

289

290 **Figure 5. Four divergent species also contain 24 nt-dominated loci that passed the three**
291 ***PHAS*-detecting algorithms.**

292 (a) Percentage of 24 nt-dominated Loci overlapping genes, transposable elements, or neither.
293 The species name is shown in the top grey boxes. P: *PHAS*-test passing locus; NP: Not *PHAS*-
294 test passing locus. For NP loci, ten cohorts of 20 randomly selected loci each were used as
295 negative controls. The number of loci in each category is shown above the bar graphs.

296 (b) Same as panel a except showing the proportion of multi-mapping reads.

297 (c) Same as panel a except showing length of the small RNA locus.

298 (d) Same as panel a except showing small RNA accumulation.

299

300 **Discussion**

301 ***rdr6*-dependent, 24 nt-dominated loci in the *A. thaliana* genome**

302 We found a handful of *rdr6*-dependent, 24 nt-dominated loci to be encoded in the *A.*
303 *thaliana* genome. However, these loci have the same genetic dependencies as hc-siRNAs
304 (Figure 4) and are frequently derived from the transposable elements (Figure S9a). The only
305 other known *rdr6*-dependent, transposon-overlapping small RNA loci encoded in *A. thaliana* are
306 epigenetically activated short interfering RNAs (easiRNAs) (Creasey et al., 2014). easiRNAs
307 are derived from transcriptionally active transposable elements that are hypothesized to be
308 targeted and cleaved by miRNAs (Creasey et al., 2014). Through the biochemical actions of
309 RDR6 and DCL4, the miRNA cleavage product is converted into 21-22 nt double-stranded RNA
310 molecules (Creasey et al., 2014). Furthermore, these easiRNAs are thought to direct initial
311 repression of transposons (He et al., 2015). It's possible that these *rdr6*-dependent, 24 nt-
312 dominated loci could represent a transitory stage of hc-siRNA targeting, in which the genetic
313 machinery of hc-siRNA are used but with a remaining initial dependency on RDR6.

314

315 **Possible losses of the *MIR2275*-generated phasing in eudicots**

316 We examined all Phytozome (ver 12.1)-curated angiosperm genomes (Goodstein et al.,
317 2012) for the presence of *MIR2275* homologs. *MIR2275* shows remarkable conservation in
318 monocots (Figure 1), showing only loss in *Musa accuminata* and *Brachypodium distachyon*.

This could be because these are aquatic plants with reduced morphology, and thus there is relaxed selective pressure for *MIR2275*. Another explanation is that the genome assemblies for these species could be incomplete. The lack of *MIR2275* in eudicots was more extensive (Figure 1), with no plants in the Brassicales clade containing a verified *MIR2275* homolog (Figure 1). Interestingly, *Aquilegia coerulea*, a basal eudicot (Sharma & Kramer, 2014), contained a *MIR2275* homolog (Figure 1; Figure S1) suggesting that the last common ancestor for eudicots may have contained *MIR2275*, and that the lack of detected putative *MIR2275* homologs in many eudicot plant species could be due to loss of *MIR2275*.

We only examined whether or not a possible *MIR2275* homolog could be detected by homology, if its predicted secondary structure is conducive to *MIRNA* processing (Figure S1), and in some species whether or not the putative *MIR2275* homolog was expressed in available small RNA libraries (Figure 1). We did not, however, determine if these species produce true 24 nt-dominated phasiRNAs. It's possible that the potential *MIR2275* homolog in these species is an orphaned *MIRNA* or has taken on a new function. Furthermore, although some putative *MIR2275* homologs had *MIRNA*-like predicted hairpins, we note that they contain mismatches in the stem of the secondary structure which may hinder miRNA biogenesis (Figure S1). Further research is necessary to determine if these species truly encode 24 nt-dominated *PHAS* loci.

The difficulties of annotating 24 nt-dominated *PHAS* loci

The discovery of 24 nt-dominated *PHAS* loci in maize (Zhai et al., 2015), rice (Song et al., 2008), asparagus, daylily, and lily (Kakrana et al., 2018) opened up the possibility that these loci exist in other species, even distantly-related eudicots. However, 24 nt-dominated hc-siRNA

loci are widespread in land plant genomes (Ghildiyal & Zamore, 2009). This is true even in *A. thaliana*, although 24 nt sRNAs are thought to repress transposable elements (Matzke et al., 2009) and only about 20-30% of the *A. thaliana* genome consists of transposon/repetitive elements (Barakat et al., 1998). In contrast, other plant genomes consist of as much as 80% transposons/repetitive elements (Springer et al., 2009). The sheer number of 24 nt-dominated sRNA loci could mean that several of them could meet various annotation criteria simply by chance; this is something we have previously noted to occur in natural antisense siRNA annotation (Polydore & Axtell, 2018).

The supposed 24 nt-dominated *PHAS* loci examined in this study consistently showed higher levels of expression than other 24 nt-dominated sRNA loci and derived from very long loci. This isn't particularly surprising because the accumulation of reads (in- and out-of-phase) is a factor in most *PHAS*-detection algorithms (Figure S3). However, it seems that particularly highly expressed 24 nt-dominated small RNAs are able to consistently pass *PHAS*-detection algorithms because of this. It's possible that the sheer number of reads produced at these loci means that these loci produce enough "in-phase" reads by chance to score highly in *PHAS*-detecting algorithms.

Annotating 24 nt-dominated *PHAS* loci in the future

Our study demonstrates that when annotating novel 24 nt-dominated *PHAS*, more than utilizing *PHAS*-detecting algorithms is necessary for robust annotation. First, examining different available mutants, especially of genes involved in small RNA biogenesis, can be critical in determining type of small RNA in question (Figure 2c). All types of phasiRNAs are known to

363 be reliant on the biochemical activity of RDR6 and Pol II (Cuperus et al., 2010; Song et al.,
364 2008; Zhai et al., 2015). While it's entirely possible that non-canonical phasiRNAs that are
365 reliant on RDR2 and Pol IV may be described eventually, such a study must verify with robust
366 methodologies that the *PHAS* loci aren't false positives due to the sheer number of Pol IV/RDR2
367 –dependent reads produced in the land plant genome.

368 We searched for *MIR2275* homologs because miR2275 is the only miRNA known to
369 trigger 24 nt phasiRNAs. If a species lacks a *MIR2275* homolog, then one should be skeptical of
370 any 24 nt-dominated small RNA locus that is annotated as *PHAS* locus in that specie. An
371 organism producing a mature miR2275 small RNA homolog is not sufficient to show that 24 nt-
372 dominated *PHAS* loci are produced in that species. One should also take care to ascertain if any
373 24 nt-dominated small RNA locus called as *PHAS* loci also contains a miR2275 target site that is
374 "in phase" with the phasiRNAs produced from the transcript. miR2275 is also very specifically
375 expressed in the tapetum of male floral tissue. In asparagus, 24 nt-dominated phasiRNAs have
376 also been shown to be expressed in female floral tissue. However, 24 nt-dominated phasiRNAs
377 have not been demonstrated to be expressed outside of reproductive tissue as of yet. Therefore,
378 any 24 nt-dominated *PHAS* loci annotated in libraries not produced from reproductive tissues are
379 more likely to be mis-annotations.

380 Despite the fact that several small RNA loci in *A. thaliana* are able to consistently pass
381 the *PHAS*-detecting algorithms in different libraries, reproducibility among distinct small RNA
382 libraries is of utmost importance. It could also be useful to employ several different *PHAS*-test
383 algorithms as well. In *A. thaliana*, three loci were able to consistently pass our *PHAS*-detecting
384 algorithms (Figure S5), but the number of loci that each algorithm detected on its own was
385 generally much higher (Figure 2a). Had we not used stringent *PHAS*-detecting methods, it

386 would've been plausible to assume we had found 24 nt-dominated *PHAS* loci in *A. thaliana*
387 based on the number of loci that consistently pass alone. Utilizing multiple small RNA libraries
388 should become easier to accomplish as more and more libraries in different treatments/genotypes
389 become available for socio-economically relevant species. Certain *PHAS*-detecting programs,
390 such as *PHASIS* (Kakrana et al., 2017), automatically evaluate potential small RNA loci in
391 different libraries individually before merging the results of each library.

392 It's not always possible to determine the small RNA that targets the phasiRNA precursor
393 transcript. Indeed, several reads may be predicted to target a certain transcript by chance due to
394 the sheer number of unique reads in a small RNA library. However, due to hydrolysis of the
395 precursor transcript following small RNA-mediated targeting, phasiRNAs have well-defined
396 termini from which they are produced (Axtell et al., 2006; Cuperus et al., 2010). Therefore, a
397 true *PHAS* loci should have a large proportion of its reads reproducibly falling into a particular
398 phase register. This is what we observed with well-characterized *PHAS* locus*, TAS2*, but not
399 with the three loci that pass our rigorous *PHAS*-annotation regime in *A. thaliana* (Figure S6).

400 As 21-22 nt-dominated *PHAS* loci are far more common in land plants, especially outside
401 of the monocots, one can conservatively limit their discovery of new *PHAS* loci to 21-22 nt-
402 dominated small RNAs and not employ as rigorous methodology as the ones used in this study.
403 However, one should still employ post *PHAS*-discovery quality controls to ensure these 21-22 nt-
404 dominated *PHAS* loci are genuine (such as determining if the predominant phase registers are
405 reproducibly dominant at these loci (Figure S6)). 24 nt-dominated *PHAS* loci on the other hand
406 seem to be have undergone loss in many angiosperms. However, even in the species in which
407 they are conserved, they seem to play very specific, reproductive-associated roles as evidenced

by their expression patterns. Great caution should be used for annotating 24 nt-dominated *PHAS* loci in the future.

Materials and Methods

Finding potential *MIR2275* homologs in angiosperms

The Phytozome (ver 12.1)-curated angiosperm genomes sequences were downloaded. The mature *O. sativa* miR2275a sequence was downloaded from miRBase (ver 21.) (Griffiths-Jones et al., 2008) and searched against all the other genomes using Bowtie v1.0 (Langmead et al., 2009) allowing for two mismatches.

In order to determine the predicted secondary structures of the Bowtie results of interest, the sequences corresponding to the Bowtie result, plus 200 nucleotides upstream and downstream, was extracted from the specie's genome. The secondary structures of the sequences were predicted using the mFOLD web server (Zuker, 2003) and visually inspected to determine if the sequence formed a hairpin structure consistent with accepted norms for miRNA biogenesis (Axtell & Meyers, 2018). The sequences were aligned using ClustalX ver. 2 with default parameters (Larkin et al., 2007).

For those species for which publicly available small RNA-seq data existed, we downloaded, trimmed, and merged the small RNA libraries. The merged libraries were collapsed to non-redundant reads and investigated using CD-HIT (ver 4.6.8) using the options -n 4, -d 0, and -g 1. The *O. sativa* miR2275a sequence was used as a query.

Determination of potential 24 nt-dominated *PHAS* loci in different wild-type, inflorescence libraries

Wild-type biological triplicate small RNA libraries (GSE105262) (Polydore & Axtell, 2018) were merged and aligned against the *A. thaliana* (TAIR 10) genome using ShortStack (ver 3.8) (Johnson et al., 2016) using 27 known *A. thaliana PHAS* loci as a query file (Table S1). Three distinct *PHAS* –detecting algorithms (Dotto et al., 2014; Johnson et al., 2016; Zheng et al., 2014) were used to determine phase scores in the merged run. These scores were used as the basis to determine cutoffs for calling significantly phased loci (Figures S3-S4). Phase scores of each known *PHAS* locus for each of the three algorithms in the eight wild-type libraries used is listed in Dataset S4. Note that we didn't use the multiple testing correction for *PHAS* loci p-values as done in Dotto et al. 2014 as we wished to test the three algorithms against each other, and the algorithms that yield phase scores couldn't be adjusted for multiple testing.

Wild-type and *rdr1-1/2-1/6-15* (*rdr1/2/6*) triple mutant small RNA libraries (GSE105262) (Polydore & Axtell, 2018) were aligned against the *A. thaliana* (TAIR 10) genome using ShortStack (ver 3.2) with option –pad 75 and option -min_cov 0.5rpm (Table S2). With these settings, small RNA loci are found as follows: All distinct genomic intervals containing one or more primary sRNA-seq alignments within 75 nts of each other were obtained, and then filtered to remove loci where the total sRNA-seq abundance with a locus was less than 0.5 reads per million. This produced a final set of distinct, non-overlapping small RNA loci. Differential expression to determine down-regulated loci was performed as previously described (Polydore & Axtell, 2018). Down-regulated, 24 nt-dominated small RNA loci were catalogued into a list. Eight wild-type, inflorescence small RNA libraries (Table S2) were run individually against the *A. thaliana* (TAIR 10) genome utilizing ShortStack (ver 3.8.1) using the results of our wild-type

and *rdr1/2/6* libraries run as a query file. The phase scores of loci corresponding to the down-regulated, 24 nt-dominated small RNAs loci were evaluated using the binary sequence alignment (BAM)-formatted alignments from each run. ShortStack and an in-house Python script was used to perform the three phase score calculations. For *B. rapa*, *C. sativus*, *P. vulgaris*, and *S. tuberosum,* the previous Shortstack merged small RNA alignments were analyzed in the same way.

For the four other species besides *A. thaliana*, we downloaded publicly available small RNA libraries (Dataset S2) for *Brassica rapa*, *Cucumis sativus*, *Phaseolus vulgaris*, and *Solanum tuberosum* and merged and aligned them against their respective genomes using ShortStack (ver 3.8.1) with default options. The genomes used were ver 1.0 for *B. rapa* (Wang et al., 2011), ver 1.0 for *P. vulgaris* (Schmutz et al., 2014), ver. 2 for *C. sativus* (Huang et al., 2009), and dm_v404 for *S. tuberosum* (Hardigan et al., 2016).

AGO Immunoprecipitation, genetic dependency, and properties of loci analyses

Calculating the lengths, proportion of multi-mapping reads, small RNA expression levels (in Reads Per Million (RPM)), determining the genetic dependencies, and the AGO enrichments of various loci were performed as previously described (Polydore & Axtell, 2018). In order to compare the properties of 24 nt-dominated loci that passed the *PHAS*-detection algorithms to those that didn't, 10 subsets of 20 loci were randomly selected from the 24 nt-dominated loci that didn't pass the *PHAS*-detection algorithms with replacement.

Examining *PHAS*-test passing loci for potential miRNA targeting

474 Sequences corresponding to the *A. thaliana* loci that consistently passed the *PHAS*-
475 detection algorithms plus 200 base pairs up-stream and downs-stream were extracted from the *A.*
476 *thaliana* genome**.** Mature miRNA sequences were downloaded from miRBase (ver 21) and
477 aligned against these sequences using the Generic Small RNA-Transcriptome Aligner. A
478 miRNA was considered to be potentially targeting a sequence if it aligned with an Allen et. al.
479 score of 3 or less.

480

481 **Acknowledgements**

482 This research was funded by NSF Award 1339207 to MJA, the NIH Bioinformatics and
483 Statistics (CBIOS) Predoctoral Training Program (1T32GM102057- 0A1) to SP, and the Henry
484 W. Popp Graduate Assistantship Fund to SP.

485

486 **Literature cited**

487 Ahmed, I., Sarazin, A., Bowler, C., Colot, V., & Quesneville, H. (2011). Genome-wide evidence
488 for local DNA methylation spreading from small RNA-targeted sequences in
489 Arabidopsis. *Nucleic Acids Research*, *39*(16), 6919–6931.
490 https://doi.org/10.1093/nar/gkr324
491 Axtell, M. J. (2010). A Method to Discover Phased siRNA Loci. In *Plant MicroRNAs* (pp. 59–
492 70). Humana Press. https://doi.org/10.1007/978-1-60327-005-2_5
493 Axtell, M. J. (2013). Classification and Comparison of Small RNAs from Plants. *Annual Review*
494 *of Plant Biology*, *64*(1), 137–159. https://doi.org/10.1146/annurev-arplant-050312-
495 120043

496 Axtell, M. J. (2015). Non-coding RNAs: The small mysteries of males. *Nature Plants*, *1*(5),
497 15055. https://doi.org/10.1038/nplants.2015.55
498 Axtell, M. J., Jan, C., Rajagopalan, R., & Bartel, D. P. (2006). A two-hit trigger for siRNA
499 biogenesis in plants. *Cell*, *127*(3), 565–577. https://doi.org/10.1016/j.cell.2006.09.032
500 Axtell, M. J., & Meyers, B. C. (2018). Revisiting criteria for plant miRNA annotation in the era
501 of big data. *The Plant Cell*, tpc.00851.2017. https://doi.org/10.1105/tpc.17.00851
502 Baev, V., Naydenov, M., Apostolova, E., Ivanova, D., Doncheva, S., Minkov, I., & Yahubyan,
503 G. (2010). Identification of RNA-dependent DNA-methylation regulated promoters in
504 Arabidopsis. *Plant Physiology and Biochemistry: PPB*, *48*(6), 393–400.
505 https://doi.org/10.1016/j.plaphy.2010.03.013
506 Barakat, A., Matassi, G., & Bernardi, G. (1998). Distribution of genes in the genome of
507 Arabidopsis thaliana and its implications for the genome organization of plants.
508 *Proceedings of the National Academy of Sciences of the United States of America*,
509 *95*(17), 10044–10049.
510 Baulcombe, D. (2004). RNA silencing in plants. *Nature*, *431*(7006), 356–363.
511 https://doi.org/10.1038/nature02874
512 Baumberger, N., & Baulcombe, D. C. (2005). Arabidopsis ARGONAUTE1 is an RNA Slicer
513 that selectively recruits microRNAs and short interfering RNAs. *Proceedings of the*
514 *National Academy of Sciences*, *102*(33), 11928–11933.
515 https://doi.org/10.1073/pnas.0505461102
516 Boualem, A., Laporte, P., Jovanovic, M., Laffont, C., Plet, J., Combier, J.-P., … Frugier, F.
517 (2008). MicroRNA166 controls root and nodule development in Medicago truncatula.

518 *The Plant Journal: For Cell and Molecular Biology*, *54*(5), 876–887.
519 https://doi.org/10.1111/j.1365-313X.2008.03448.x
520 Chapman, E. J., & Carrington, J. C. (2007). Specialization and evolution of endogenous small
521 RNA pathways. *Nature Reviews Genetics*, *8*(11), 884–896.
522 https://doi.org/10.1038/nrg2179
523 Creasey, K. M., Zhai, J., Borges, F., Van Ex, F., Regulski, M., Meyers, B. C., & Martienssen, R.
524 A. (2014). miRNAs trigger widespread epigenetically activated siRNAs from transposons
525 in Arabidopsis. *Nature*, *508*(7496), 411–415. https://doi.org/10.1038/nature13069
526 Cuperus, J. T., Carbonell, A., Fahlgren, N., Garcia-Ruiz, H., Burke, R. T., Takeda, A., …
527 Carrington, J. C. (2010). Unique functionality of 22-nt miRNAs in triggering RDR6-
528 dependent siRNA biogenesis from target transcripts in *Arabidopsis*. *Nature Structural &*
529 *Molecular Biology*, *17*(8), 997–1003. https://doi.org/10.1038/nsmb.1866
530 Dotto, M. C., Petsch, K. A., Aukerman, M. J., Beatty, M., Hammell, M., & Timmermans, M. C.
531 P. (2014). Genome-Wide Analysis of leafbladeless1-Regulated and Phased Small RNAs
532 Underscores the Importance of the TAS3 ta-siRNA Pathway to Maize Development.
533 *PLOS Genetics*, *10*(12), e1004826. https://doi.org/10.1371/journal.pgen.1004826
534 Elvira-Matelot, E., Hachet, M., Shamandi, N., Comella, P., Sáez-Vásquez, J., Zytnicki, M., &
535 Vaucheret, H. (2016). Arabidopsis RNASE THREE LIKE2 Modulates the Expression of
536 Protein-Coding Genes via 24-Nucleotide Small Interfering RNA-Directed DNA
537 Methylation. *The Plant Cell Online*, *28*(2), 406–425.
538 https://doi.org/10.1105/tpc.15.00540
539 Ender, C., & Meister, G. (2010). Argonaute proteins at a glance. *J Cell Sci*, *123*(11), 1819–1823.
540 https://doi.org/10.1242/jcs.055210

541 Fei, Q., Xia, R., & Meyers, B. C. (2013). Phased, Secondary, Small Interfering RNAs in
542 Posttranscriptional Regulatory Networks. *The Plant Cell Online*, *25*(7), 2400–2415.
543 https://doi.org/10.1105/tpc.113.114652
544 Gasciolli, V., Mallory, A. C., Bartel, D. P., & Vaucheret, H. (2005). Partially Redundant
545 Functions of Arabidopsis DICER-like Enzymes and a Role for DCL4 in Producing trans-
546 Acting siRNAs. *Current Biology*, *15*(16), 1494–1500.
547 https://doi.org/10.1016/j.cub.2005.07.024
548 Ghildiyal, M., & Zamore, P. D. (2009). Small silencing RNAs: an expanding universe. *Nature*
549 *Reviews. Genetics*, *10*(2), 94–108. https://doi.org/10.1038/nrg2504
550 Goodstein, D. M., Shu, S., Howson, R., Neupane, R., Hayes, R. D., Fazo, J., … Rokhsar, D. S.
551 (2012). Phytozome: a comparative platform for green plant genomics. *Nucleic Acids*
552 *Research*, *40*(Database issue), D1178–D1186. https://doi.org/10.1093/nar/gkr944
553 Grant-Downton, R., Hafidh, S., Twell, D., & Dickinson, H. G. (2009). Small RNA Pathways Are
554 Present and Functional in the Angiosperm Male Gametophyte. *Molecular Plant*, *2*(3),
555 500–512. https://doi.org/10.1093/mp/ssp003
556 Griffiths-Jones, S., Saini, H. K., van Dongen, S., & Enright, A. J. (2008). miRBase: tools for
557 microRNA genomics. *Nucleic Acids Research*, *36*(suppl_1), D154–D158.
558 https://doi.org/10.1093/nar/gkm952
559 Groth, M., Stroud, H., Feng, S., Greenberg, M. V. C., Vashisht, A. A., Wohlschlegel, J. A., …
560 Ausin, I. (2014). SNF2 chromatin remodeler-family proteins FRG1 and -2 are required
561 for RNA-directed DNA methylation. *Proceedings of the National Academy of Sciences of*
562 *the United States of America*, *111*(49), 17666–17671.
563 https://doi.org/10.1073/pnas.1420515111

564 Guo, Q., Qu, X., & Jin, W. (2015). PhaseTank: genome-wide computational identification of
565 phasiRNAs and their regulatory cascades. *Bioinformatics*, *31*(2), 284–286.
566 https://doi.org/10.1093/bioinformatics/btu628
567 Hardigan, M. A., Crisovan, E., Hamiltion, J. P., Kim, J., Laimbeer, P., Leisner, C. P., … Buell,
568 C. R. (2016). Genome reduction uncovers a large dispensable genome and adaptive role
569 for copy number variation in asexually propagated Solanum tuberosum. *The Plant Cell*,
570 TPC2015–00538–RA. https://doi.org/10.1105/tpc.15.00538
571 He, H., Yang, T., Wu, W., & Zheng, B. (2015). Small RNAs in pollen. *Science China Life*
572 *Sciences*, *58*(3), 246–252. https://doi.org/10.1007/s11427-015-4800-0
573 Huang, S., Li, R., Zhang, Z., Li, L., Gu, X., Fan, W., … Li, S. (2009). The genome of the
574 cucumber, *Cucumis sativus* L. *Nature Genetics*, *41*(12), 1275–1281.
575 https://doi.org/10.1038/ng.475
576 Jeong, D.-H., Thatcher, S. R., Brown, R. S. H., Zhai, J., Park, S., Rymarquis, L. A., … Green, P.
577 J. (2013). Comprehensive Investigation of MicroRNAs Enhanced by Analysis of
578 Sequence Variants, Expression Patterns, ARGONAUTE Loading, and Target
579 Cleavage1[W][OA]. *Plant Physiology*, *162*(3), 1225–1245.
580 https://doi.org/10.1104/pp.113.219873
581 Johnson, N. R., Yeoh, J. M., Coruh, C., & Axtell, M. J. (2016). Improved Placement of Multi-
582 mapping Small RNAs. *G3: Genes, Genomes, Genetics*, *6*(7), 2103–2111.
583 https://doi.org/10.1534/g3.116.030452
584 Kakrana, A., Li, P., Patel, P., Hammond, R., Anand, D., Mathioni, S., & Meyers, B. (2017).
585 PHASIS: A computational suite for de novo discovery and characterization of phased,

586 siRNA-generating loci and their miRNA triggers. *bioRxiv*, 158832.
587 https://doi.org/10.1101/158832
588 Kakrana, A., Mathioni, S. M., Huang, K., Hammond, R., Vandivier, L., Patel, P., … Meyers, B.
589 C. (2018). Plant 24-nt reproductive phasiRNAs from intramolecular duplex mRNAs in
590 diverse monocots. *Genome Research*, gr.228163.117.
591 https://doi.org/10.1101/gr.228163.117
592 Komiya, R., Ohyanagi, H., Niihama, M., Watanabe, T., Nakano, M., Kurata, N., & Nonomura,
593 K.-I. (2014). Rice germline-specific Argonaute MEL1 protein binds to phasiRNAs
594 generated from more than 700 lincRNAs. *The Plant Journal*, *78*(3), 385–397.
595 https://doi.org/10.1111/tpj.12483
596 Kumar, S., Stecher, G., Suleski, M., & Hedges, S. B. (2017). TimeTree: A Resource for
597 Timelines, Timetrees, and Divergence Times. *Molecular Biology and Evolution*, *34*(7),
598 1812–1819. https://doi.org/10.1093/molbev/msx116
599 Kutter, C., Schöb, H., Stadler, M., Meins, F., & Si-Ammour, A. (2007). MicroRNA-Mediated
600 Regulation of Stomatal Development in Arabidopsis. *The Plant Cell*, *19*(8), 2417–2429.
601 https://doi.org/10.1105/tpc.107.050377
602 Langmead, B., Trapnell, C., Pop, M., & Salzberg, S. L. (2009). Ultrafast and memory-efficient
603 alignment of short DNA sequences to the human genome. *Genome Biology*, *10*(3), R25.
604 https://doi.org/10.1186/gb-2009-10-3-r25
605 Larkin, M. A., Blackshields, G., Brown, N. P., Chenna, R., McGettigan, P. A., McWilliam, H.,
606 … Higgins, D. G. (2007). Clustal W and Clustal X version 2.0. *Bioinformatics*, *23*(21),
607 2947–2948. https://doi.org/10.1093/bioinformatics/btm404

608 Laufs, P., Peaucelle, A., Morin, H., & Traas, J. (2004). MicroRNA regulation of the CUC genes
609 is required for boundary size control in Arabidopsis meristems. *Development*, *131*(17),
610 4311–4322. https://doi.org/10.1242/dev.01320
611 Lee, T., Gurazada, S. G. R., Zhai, J., Li, S., Simon, S. A., Matzke, M. A., … Meyers, B. C.
612 (2012). RNA polymerase V-dependent small RNAs in Arabidopsis originate from small,
613 intergenic loci including most SINE repeats. *Epigenetics*, *7*(7), 781–795.
614 https://doi.org/10.4161/epi.20290
615 Li, S., Vandivier, L. E., Tu, B., Gao, L., Won, S. Y., Li, S., … Chen, X. (2014). Detection of Pol
616 IV/RDR2-dependent transcripts at the genomic scale in Arabidopsis reveals features and
617 regulation of siRNA biogenesis. *Genome Research*, gr.182238.114.
618 https://doi.org/10.1101/gr.182238.114
619 Matzke, M., Kanno, T., Daxinger, L., Huettel, B., & Matzke, A. J. (2009). RNA-mediated
620 chromatin-based silencing in plants. *Current Opinion in Cell Biology*, *21*(3), 367–376.
621 https://doi.org/10.1016/j.ceb.2009.01.025
622 Mi, S., Cai, T., Hu, Y., Chen, Y., Hodges, E., Ni, F., … Qi, Y. (2008). Sorting of Small RNAs
623 into Arabidopsis Argonaute Complexes Is Directed by the 5′ Terminal Nucleotide. *Cell*,
624 *133*(1), 116–127. https://doi.org/10.1016/j.cell.2008.02.034
625 Millar, A. A., & Waterhouse, P. M. (2005). Plant and animal microRNAs: similarities and
626 differences. *Functional & Integrative Genomics*, *5*(3), 129–135.
627 https://doi.org/10.1007/s10142-005-0145-2
628 Ono, S., Liu, H., Tsuda, K., Fukai, E., Tanaka, K., Sasaki, T., & Nonomura, K.-I. (2018). EAT1
629 transcription factor, a non-cell-autonomous regulator of pollen production, activates

meiotic small RNA biogenesis in rice anther tapetum. *PLOS Genetics*, *14*(2), e1007238. https://doi.org/10.1371/journal.pgen.1007238

Onodera, Y., Haag, J. R., Ream, T., Nunes, P. C., Pontes, O., & Pikaard, C. S. (2005). Plant Nuclear RNA Polymerase IV Mediates siRNA and DNA Methylation-Dependent Heterochromatin Formation. *Cell*, *120*(5), 613–622. https://doi.org/10.1016/j.cell.2005.02.007

Panda, K., Ji, L., Neumann, D. A., Daron, J., Schmitz, R. J., & Slotkin, R. K. (2016). Full-length autonomous transposable elements are preferentially targeted by expression-dependent forms of RNA-directed DNA methylation. *Genome Biology*, *17*, 170. https://doi.org/10.1186/s13059-016-1032-y

Polydore, S., & Axtell, M. J. (2018). Analysis of RDR1/RDR2/RDR6-independent small RNAs in Arabidopsis thaliana improves MIRNA annotations and reveals unexplained types of short interfering RNA loci. *The Plant Journal: For Cell and Molecular Biology*, *94*(6), 1051–1063. https://doi.org/10.1111/tpj.13919

Qi, Y., Denli, A. M., & Hannon, G. J. (2005). Biochemical Specialization within Arabidopsis RNA Silencing Pathways. *Molecular Cell*, *19*(3), 421–428. https://doi.org/10.1016/j.molcel.2005.06.014

Schmutz, J., McClean, P. E., Mamidi, S., Wu, G. A., Cannon, S. B., Grimwood, J., … Jackson, S. A. (2014). A reference genome for common bean and genome-wide analysis of dual domestications. *Nature Genetics*, *46*(7), 707–713. https://doi.org/10.1038/ng.3008

Sharma, B., & Kramer, E. M. (2014). THE MADS-BOX GENE FAMILY OF THE BASAL EUDICOT AND HYBRID AQUILEGIA COERULEA “ORIGAMI” (RANUNCULACEAE). *Annals of the Missouri Botanical Garden*, *99*(3), 313–322.

653 Song, X., Li, P., Zhai, J., Zhou, M., Ma, L., Liu, B., … Cao, X. (2008). Roles of DCL4 and
654 DCL3b in rice phased small RNA biogenesis. *The Plant Journal*, *69*(3), 462–474.
655 https://doi.org/10.1111/j.1365-313X.2011.04805.x
656 Springer, N. M., Ying, K., Fu, Y., Ji, T., Yeh, C.-T., Jia, Y., … Schnable, P. S. (2009). Maize
657 Inbreds Exhibit High Levels of Copy Number Variation (CNV) and Presence/Absence
658 Variation (PAV) in Genome Content. *PLOS Genetics*, *5*(11), e1000734.
659 https://doi.org/10.1371/journal.pgen.1000734
660 Sugiyama, T., Cam, H., Verdel, A., Moazed, D., & Grewal, S. I. S. (2005). RNA-dependent
661 RNA polymerase is an essential component of a self-enforcing loop coupling
662 heterochromatin assembly to siRNA production. *Proceedings of the National Academy of*
663 *Sciences of the United States of America*, *102*(1), 152.
664 https://doi.org/10.1073/pnas.0407641102
665 Tamim, S., Cai, Z., Mathioni, S., Zhai, J., Teng, C., Zhang, Q., & Meyers, B. C. (2018). Cis-
666 directed cleavage and nonstoichiometric abundances of 21-nt reproductive phasiRNAs in
667 grasses. *bioRxiv*, 243907. https://doi.org/10.1101/243907
668 Tolia, N. H., & Joshua-Tor, L. (2007). Slicer and the Argonautes. *Nature Chemical Biology*,
669 *3*(1), 36–43. https://doi.org/10.1038/nchembio848
670 Wang, X., Wang, H., Wang, J., Sun, R., Wu, J., Liu, S., … Zhang, Z. (2011). The genome of the
671 mesopolyploid crop species *Brassica rapa*. *Nature Genetics*, *43*(10), 1035–1039.
672 https://doi.org/10.1038/ng.919
673 Williams, L., Grigg, S. P., Xie, M., Christensen, S., & Fletcher, J. C. (2005). Regulation of
674 Arabidopsis shoot apical meristem and lateral organ formation by microRNA miR166g

675 and its AtHD-ZIP target genes. *Development*, *132*(16), 3657–3668.
676 https://doi.org/10.1242/dev.01942
677 Willmann, M. R., Endres, M. W., Cook, R. T., & Gregory, B. D. (2011). The Functions of RNA-
678 Dependent RNA Polymerases in Arabidopsis. *The Arabidopsis Book*, e0146.
679 https://doi.org/10.1199/tab.0146
680 Ye, R., Chen, Z., Lian, B., Rowley, M. J., Xia, N., Chai, J., … Qi, Y. (2016). A Dicer-
681 Independent Route for Biogenesis of siRNAs that Direct DNA Methylation in
682 Arabidopsis. *Molecular Cell*, *61*(2), 222–235.
683 https://doi.org/10.1016/j.molcel.2015.11.015
684 Zhai, J., Bischof, S., Wang, H., Feng, S., Lee, T., Teng, C., … Jacobsen, S. E. (2015). One
685 precursor One siRNA model for Pol IV- dependent siRNAs Biogenesis. *Cell*, *163*(2),
686 445–455. https://doi.org/10.1016/j.cell.2015.09.032
687 Zhai, J., Zhang, H., Arikit, S., Huang, K., Nan, G.-L., Walbot, V., & Meyers, B. C. (2015).
688 Spatiotemporally dynamic, cell-type–dependent premeiotic and meiotic phasiRNAs in
689 maize anthers. *Proceedings of the National Academy of Sciences*, *112*(10), 3146–3151.
690 https://doi.org/10.1073/pnas.1418918112
691 Zhang, H., Xia, R., Meyers, B. C., & Walbot, V. (2015). Evolution, functions, and mysteries of
692 plant ARGONAUTE proteins. *Current Opinion in Plant Biology*, *27*, 84–90.
693 https://doi.org/10.1016/j.pbi.2015.06.011
694 Zheng, Yi, Wang, Y., Wu, J., Ding, B., & Fei, Z. (2015). A dynamic evolutionary and functional
695 landscape of plant phased small interfering RNAs. *BMC Biology*, *13*.
696 https://doi.org/10.1186/s12915-015-0142-4

Zheng, Yun, Wang, S., & Sunkar, R. (2014). Genome-Wide Discovery and Analysis of Phased Small Interfering RNAs in Chinese Sacred Lotus. *PLoS ONE*, *9*(12). https://doi.org/10.1371/journal.pone.0113790

Zuker, M. (2003). Mfold web server for nucleic acid folding and hybridization prediction. *Nucleic Acids Research*, *31*(13), 3406–3415.

Supplementary Figures

Eudicots

Citrus sinensis (Sweet Orange)

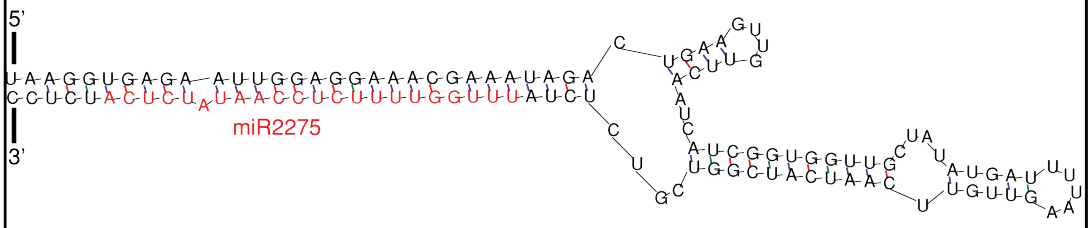

Scaffold02893:5,816-6,237

Citrus clementina (Clementine)

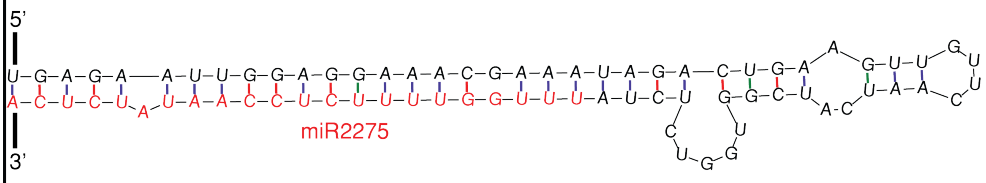

Scaffold_7:11,677,716-11,678,137

Populus trichocarpa (Black Cottonwood)

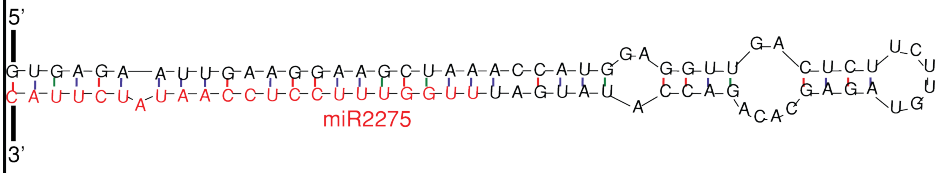

Chr18:16,602,794-16,603,213

Fragaria vesca (Woodland Stawberry)

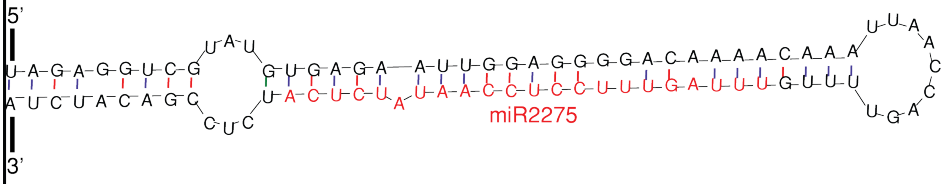

LG6:33,999,807-34,000,228

712

Prunus persica (Peach)

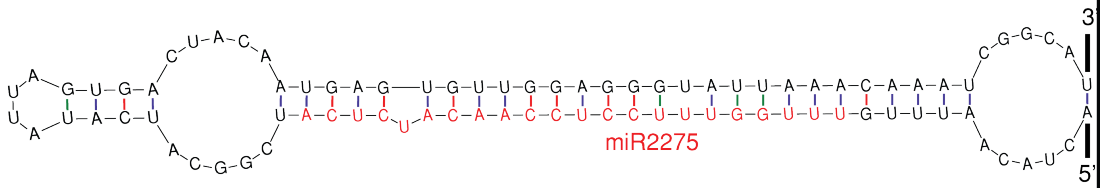

Pp03:25,091,557-25,091,979

Daucus carota (Carrot)

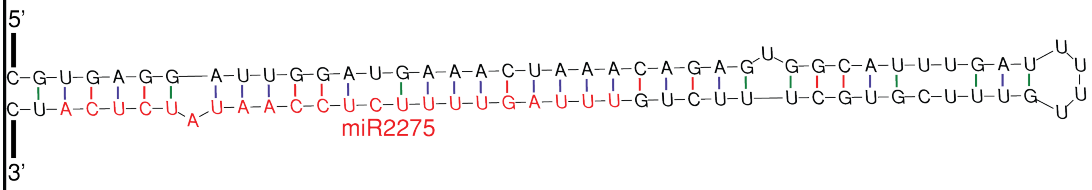

DCARv2_Chr3:50,126,000-50,126,421

Linum usitatissimum (Flax)

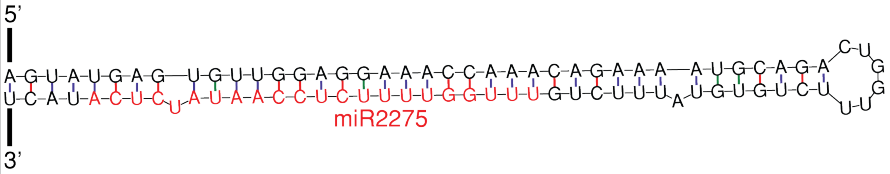

Scaffold917:325,461-325,882

Salix purpurea

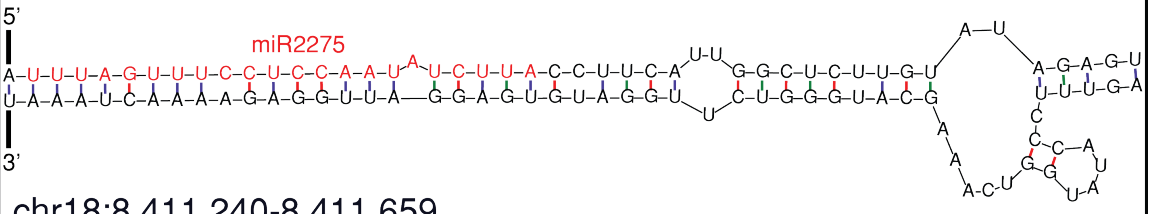

chr18:8,411,240-8,411,659

713

Manihot esculenta (Cassava)

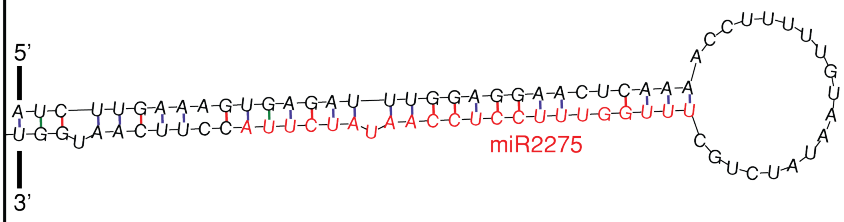

Chromosome09:25,243,068-25,243,487

Vitis vinifera (Grapevine)

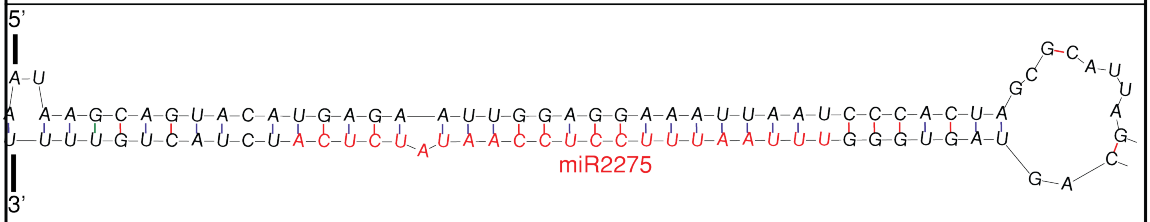

Chr1:11,599,187-11,599,609

Aquilegia coerulea

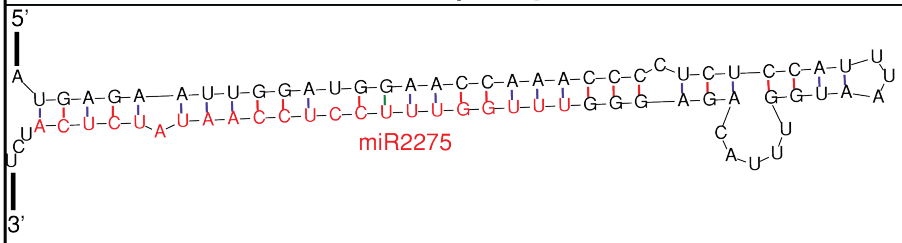

Chr5:8,028,124-8,028,545

Malus domestica (Apple)

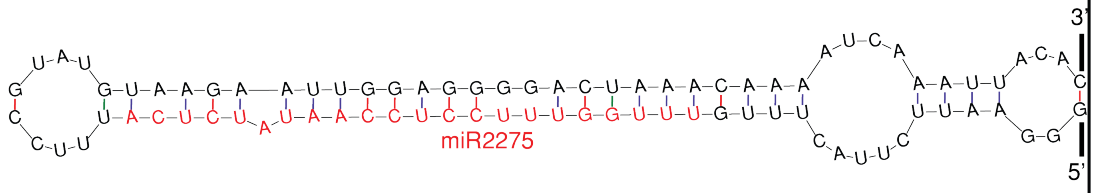

MDC013357.204:1,230-1,652

714

Monocots

Panicum hallii

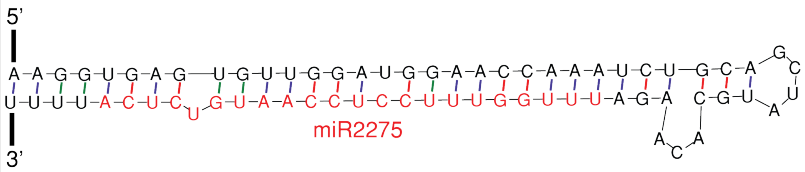

chr18_random:2,094,218-2,094,599

Ananas comosus (Pineapple)

LG24:194,094-194,515

Brachypodium distachyon

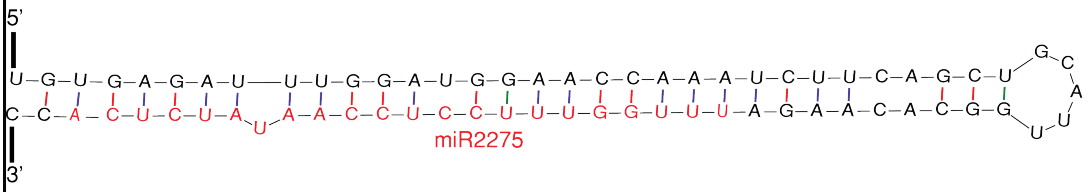

Bd3:12,534,229-12,534,651

Setaria viridis

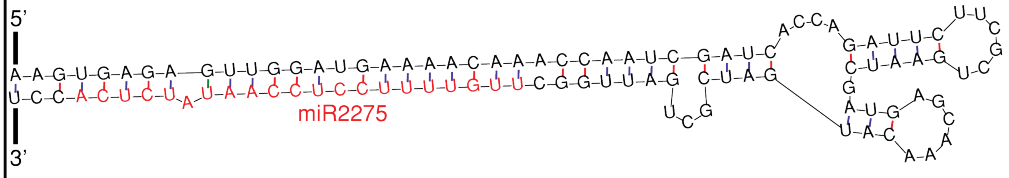

Chr_06:3,634,546-3,634,966

715

Zea mays (Maize)

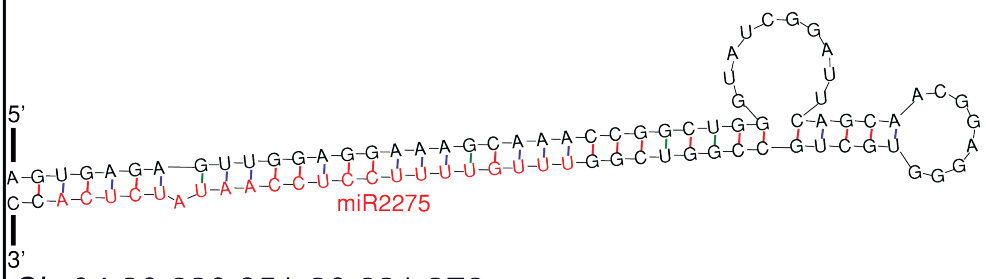

Chr04:30,230,951-30,231,372

Sorghum bicolor

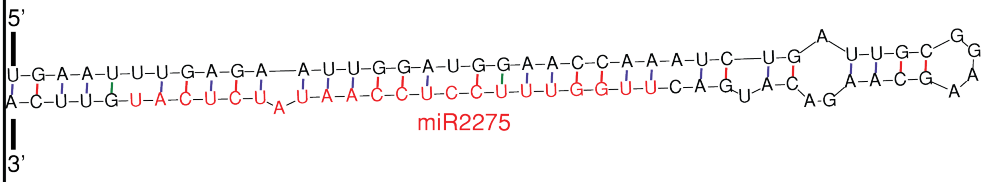

Chr07:2,205,924-2,206,344

Panicum virgatum (Switchgrass)

Chr06N:2,434,933-2,435,354

Oropetium thomaeum

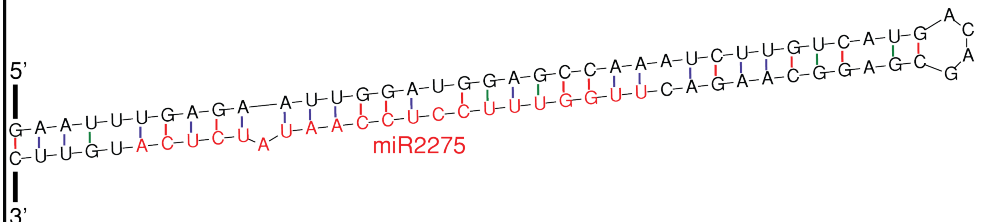

Oropetium_genomic_20141112_019:926,647-927,067

716

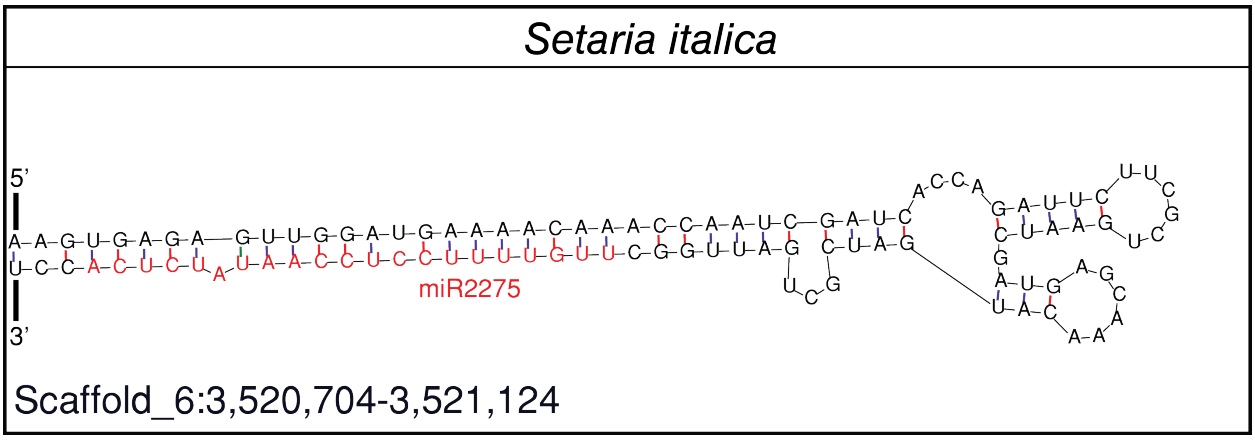

Figure S1. The RNA secondary structure of Bowtie-validated *MIR2275* homologs.

Secondary structures of loci were predicted via mFOLD. If the potential *MIR2275* homolog formed a stem-and-loop structure, it is shown above. The red nucleotides denote the mature *MIR2275* homolog in the secondary structure.

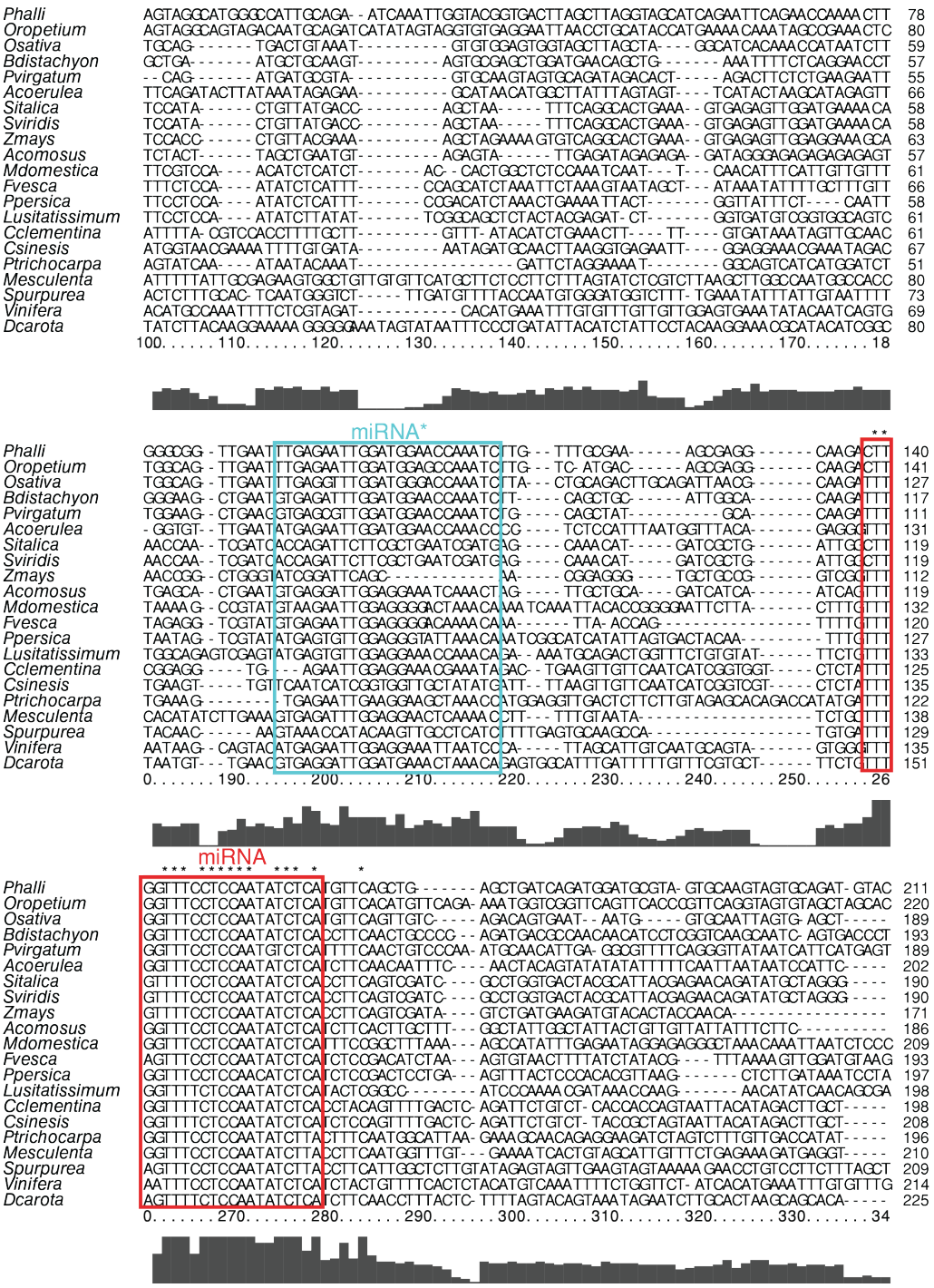

Figure S2. Alignment of *MIR2275* homologs.

Sequences corresponding to miR2275 wih flanking 200 bp islands were extracted from genomes of the above-listed genomes and aligned via ClustalX2. Only the 100th to 340th nucleotide of each sequence (including gaps) are shown. miR2275 and miR2275* in each species are shown.

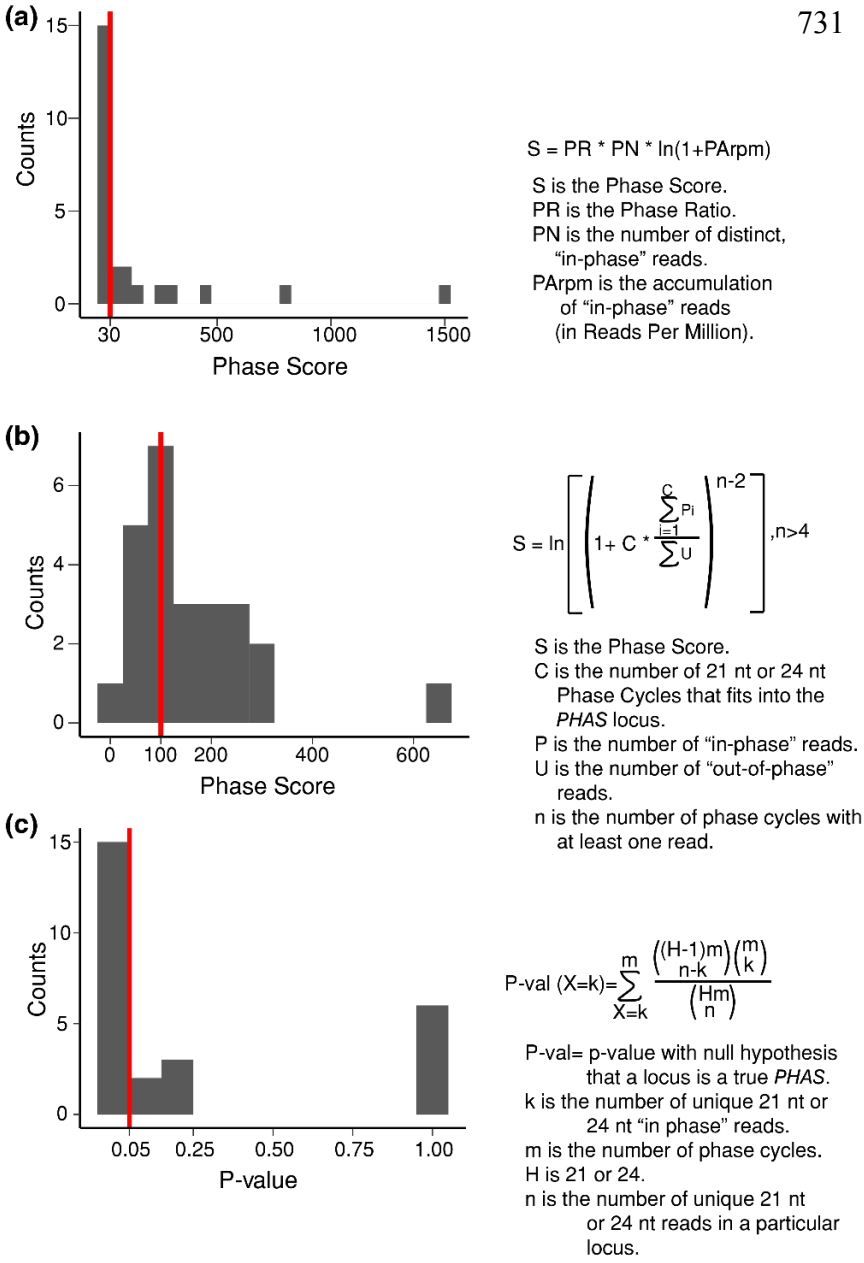

732

733 **Figure S3. Determination of phase score cutoffs using three different algorithms**

734 (a) Small RNA accumulation at 27 known 21 nt *PHAS* loci (Table S1) was analyzed using the
735 *PHAS*-Test algorithm from Guo et al. (2015), which is used by ShortStack. Variables and
736 formula are shown. Red line represents the cut-off used in this study to determine if a locus was
737 phased or not; scores above the red line were considered 'phased'.

738 (b) Same as in panel a except for the *PHAS*-Test algorithm from Dotto et al. (2014).

739 (c) Same as in panel a except for the *PHAS*-Test algorithm from Zheng et al. (2014); scores
740 below the red-line were considered 'phased'.

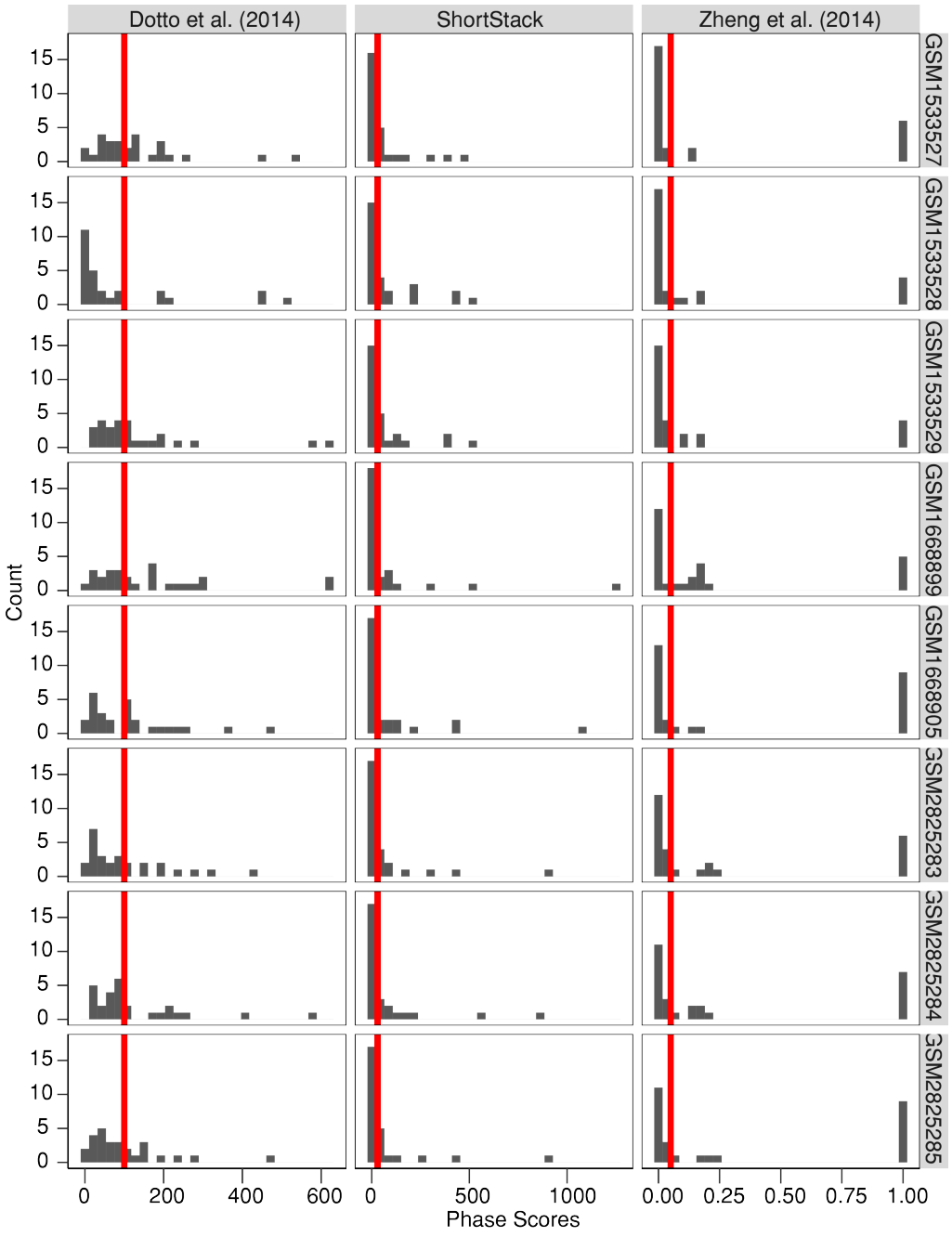

741

742 **Figure S4.** Phase scores of 27 previously known *A. thaliana* phased siRNA loci from the
743 indicated algorithms. Cutoff values for called 'phasing' in our study are shown in red.

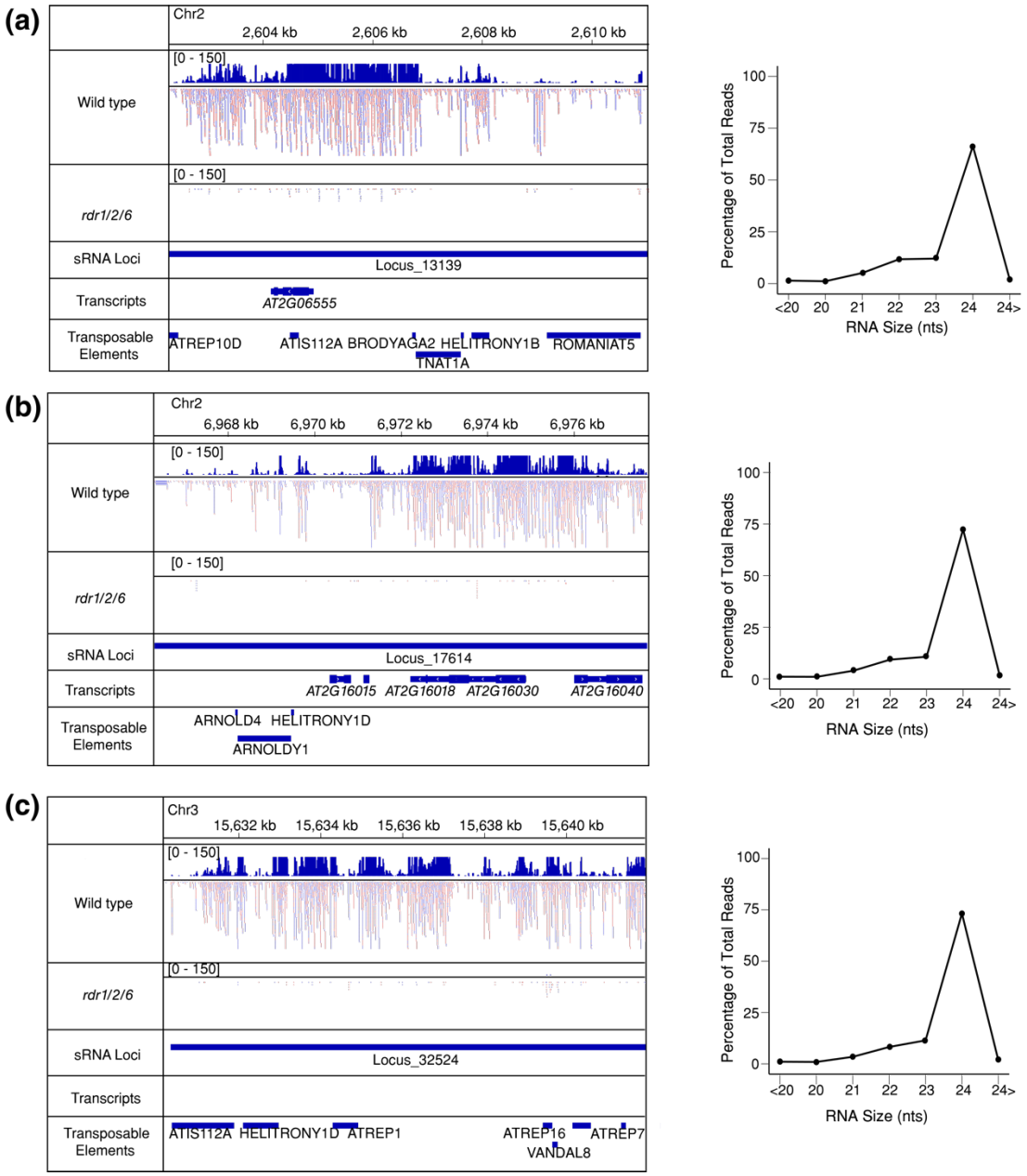

744

745 **Figure S5. Genome browser snapshots of the three *Arabidopsis thaliana PHAS*-Test**
746 **passing loci.**

747 (a) Alignments and read size distribution of Locus_13139. Red reads represent positive-strand
748 mapped genes, while blue reads are those that mapped to the negative strand. Numbers in the
749 brackets are the range of coverage shown in Reads per Million.

750 (b) Same as a, except for Locus_17614.

751 (c) Same as a, except for Locus_32524.

Locus_13139

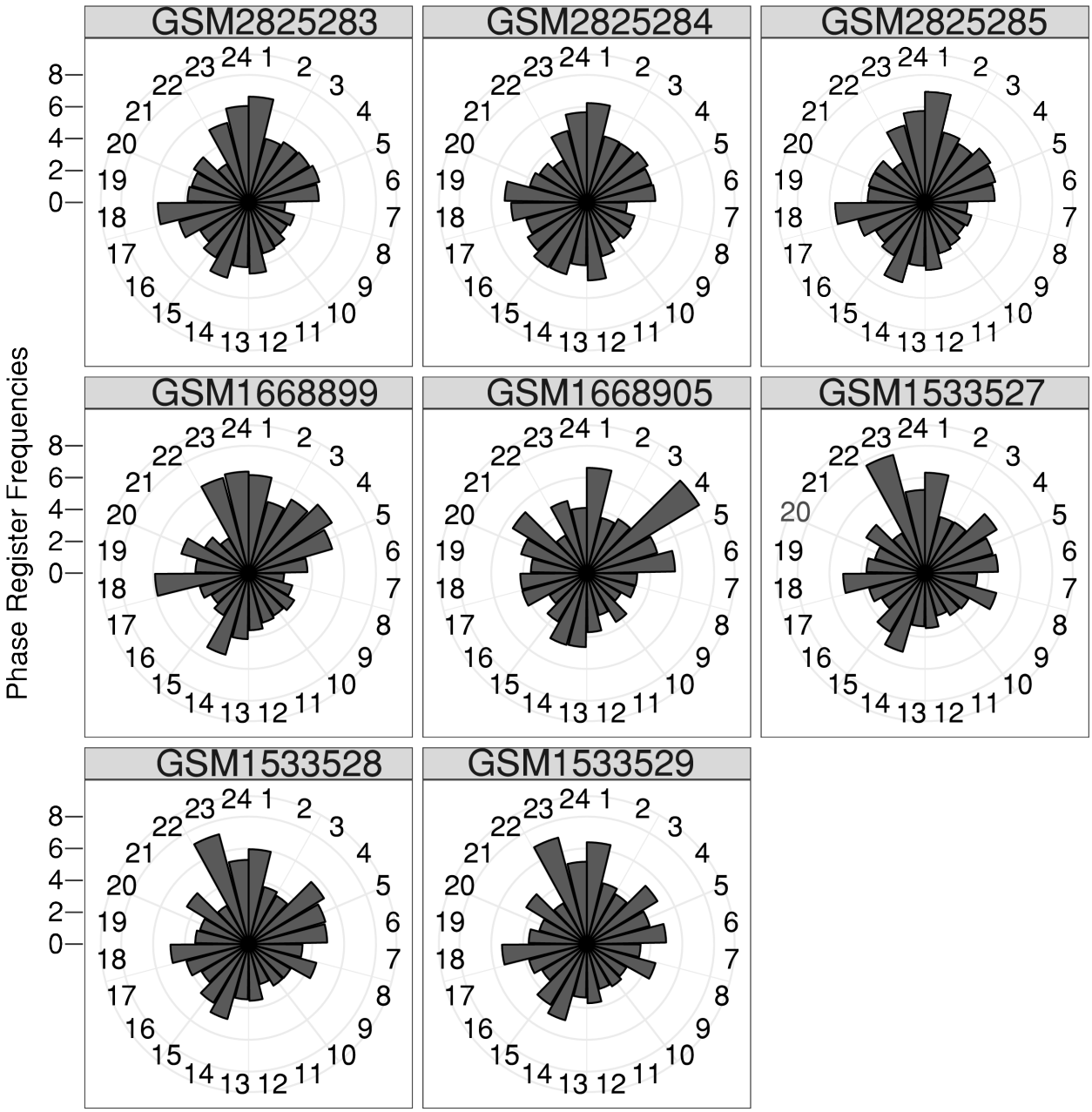

752

753

Locus_17614

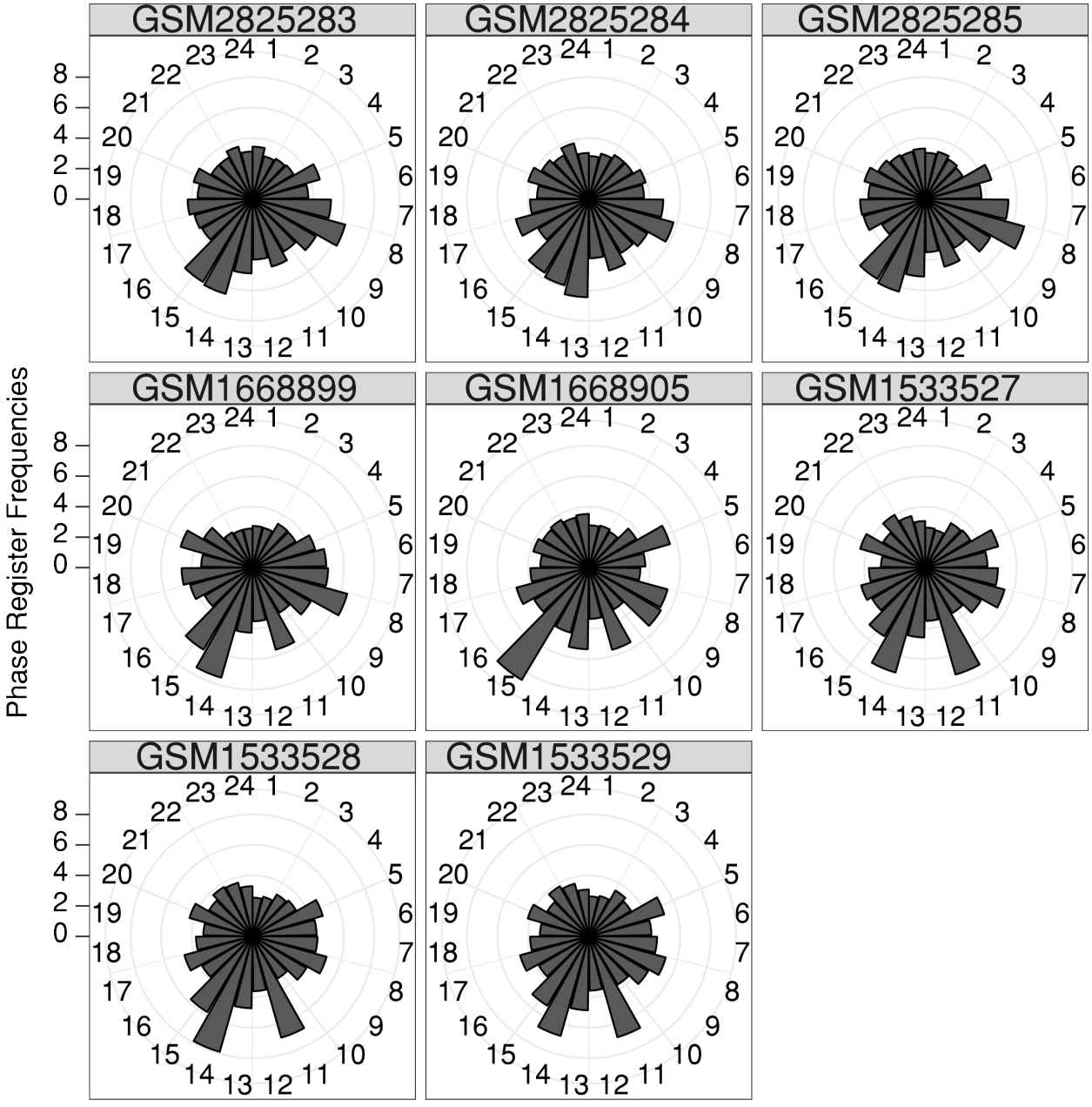

754

755

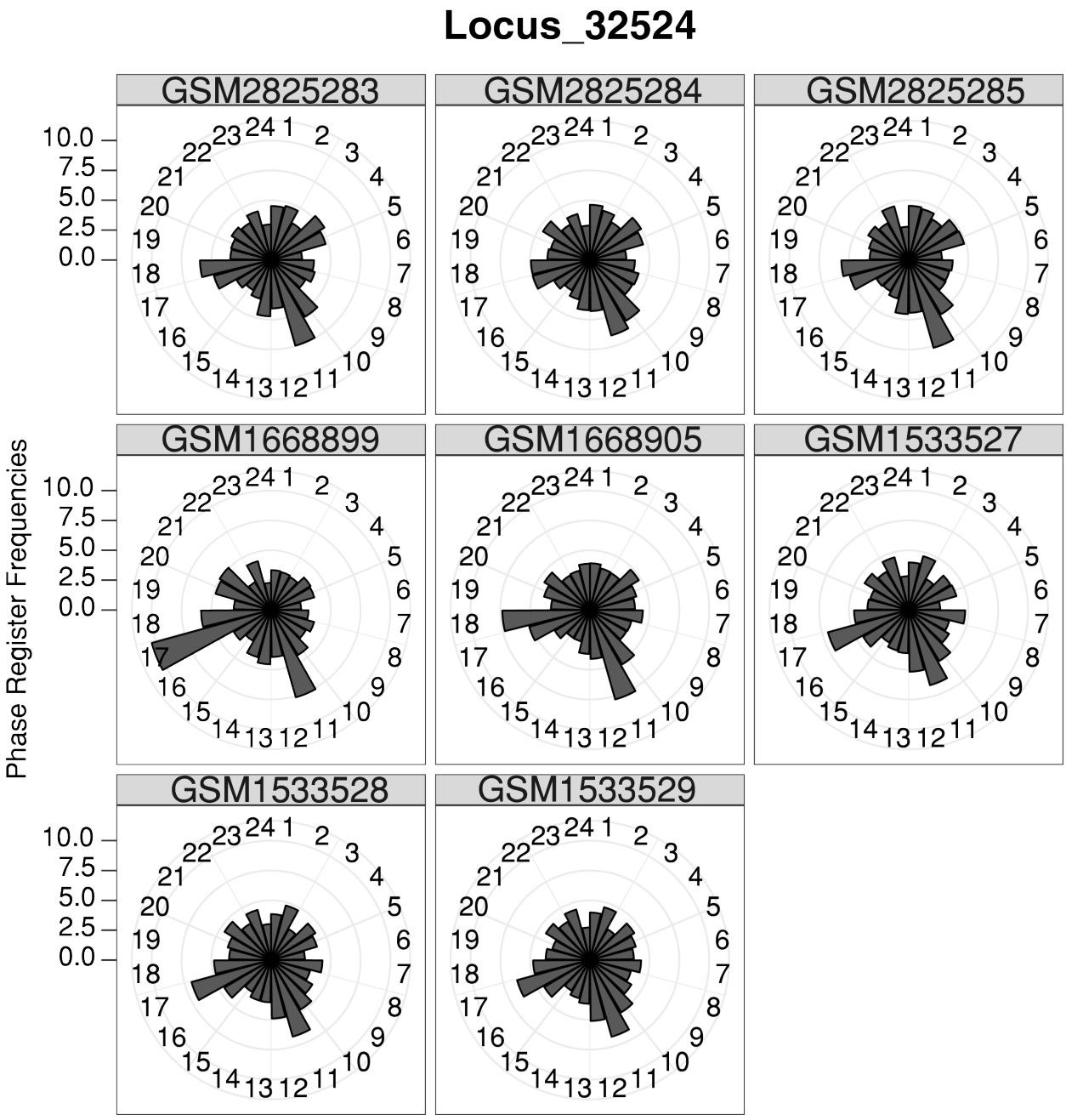

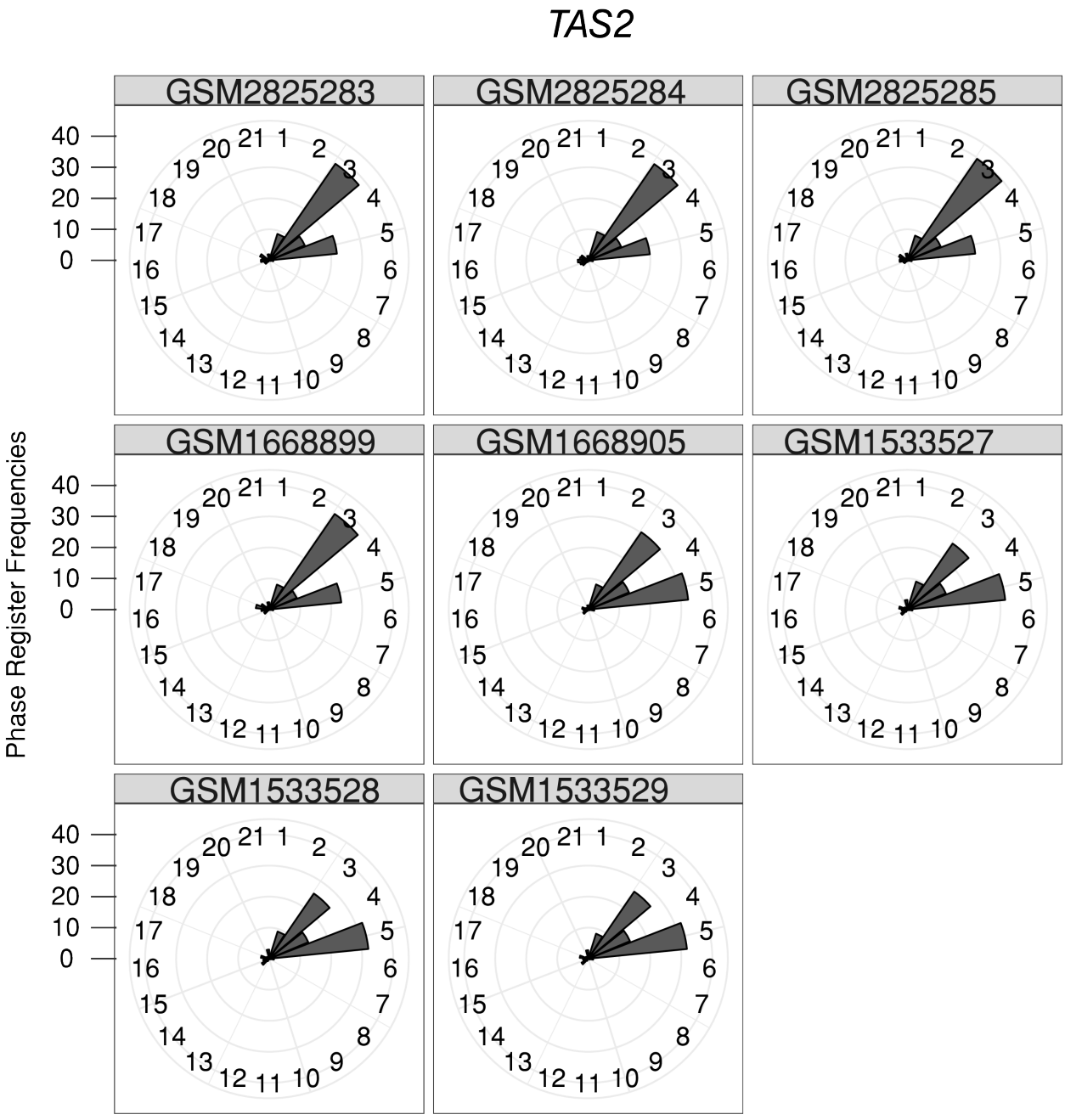

Figure S6. The three *PHAS*-Test passing loci have inconsistent phase register frequencies.

Frequencies of phase registers where calculated in eight publicly available wild-type inflorescence libraries from *A. thaliana* (the accession numbers are listed in the grey boxes). *TAS2* is shown for comparison. Phase register frequencies are calculated via the following formula: (number of reads "in phase"/ total number of reads at locus)*100.

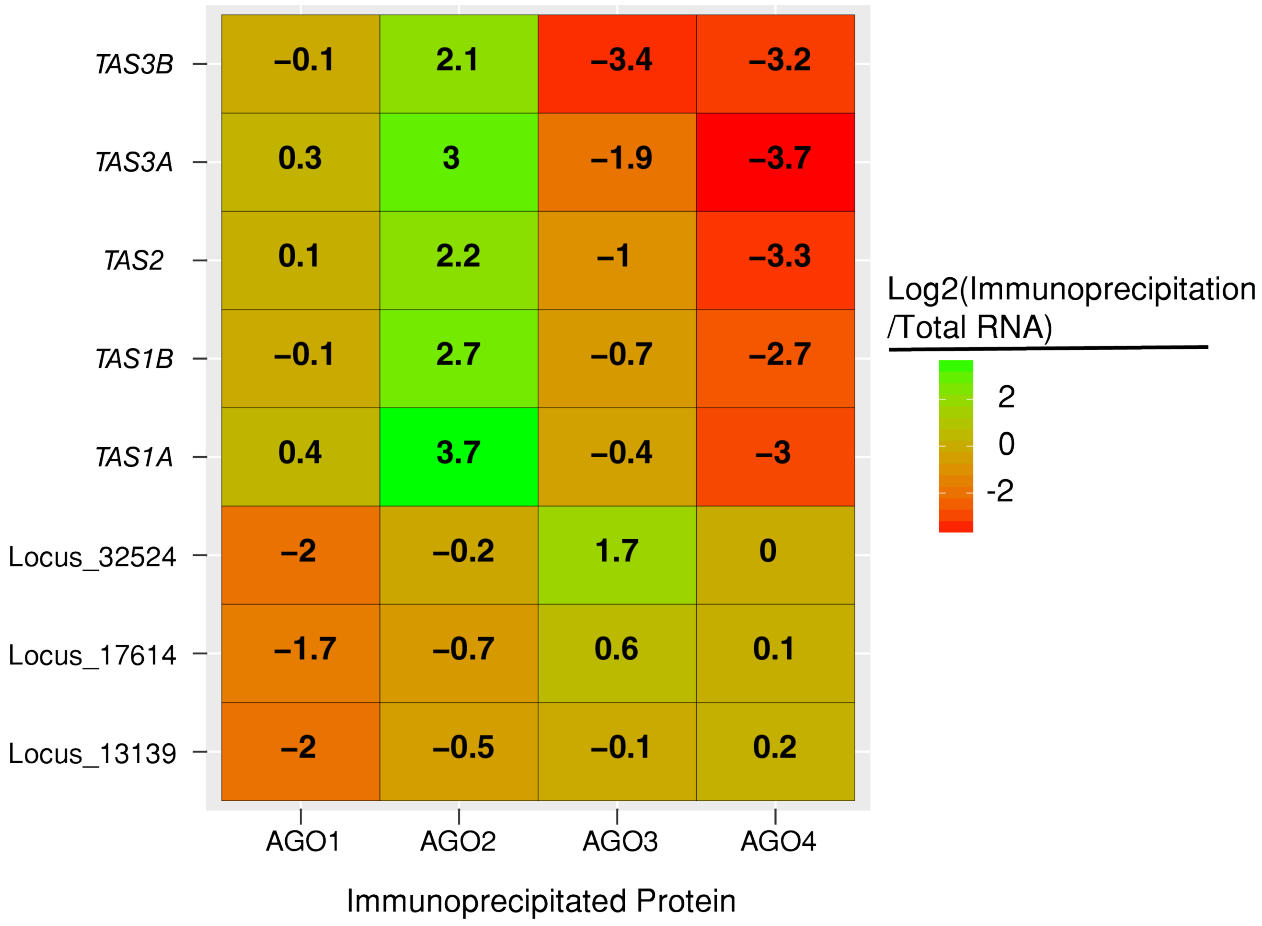

764

765 **Figure S7. The three putative 24 nt *PHAS* loci show AGO-loading profiles that are distinct**
766 **from *TAS* loci.**

767 Small RNAs from immunoprecipitation protein were aligned to the *A. thaliana* (TAIR10)
768 genome. Numbers indicate the ratio of sRNA accumulation between immunoprecipitated and
769 total libraries (in RPMs).

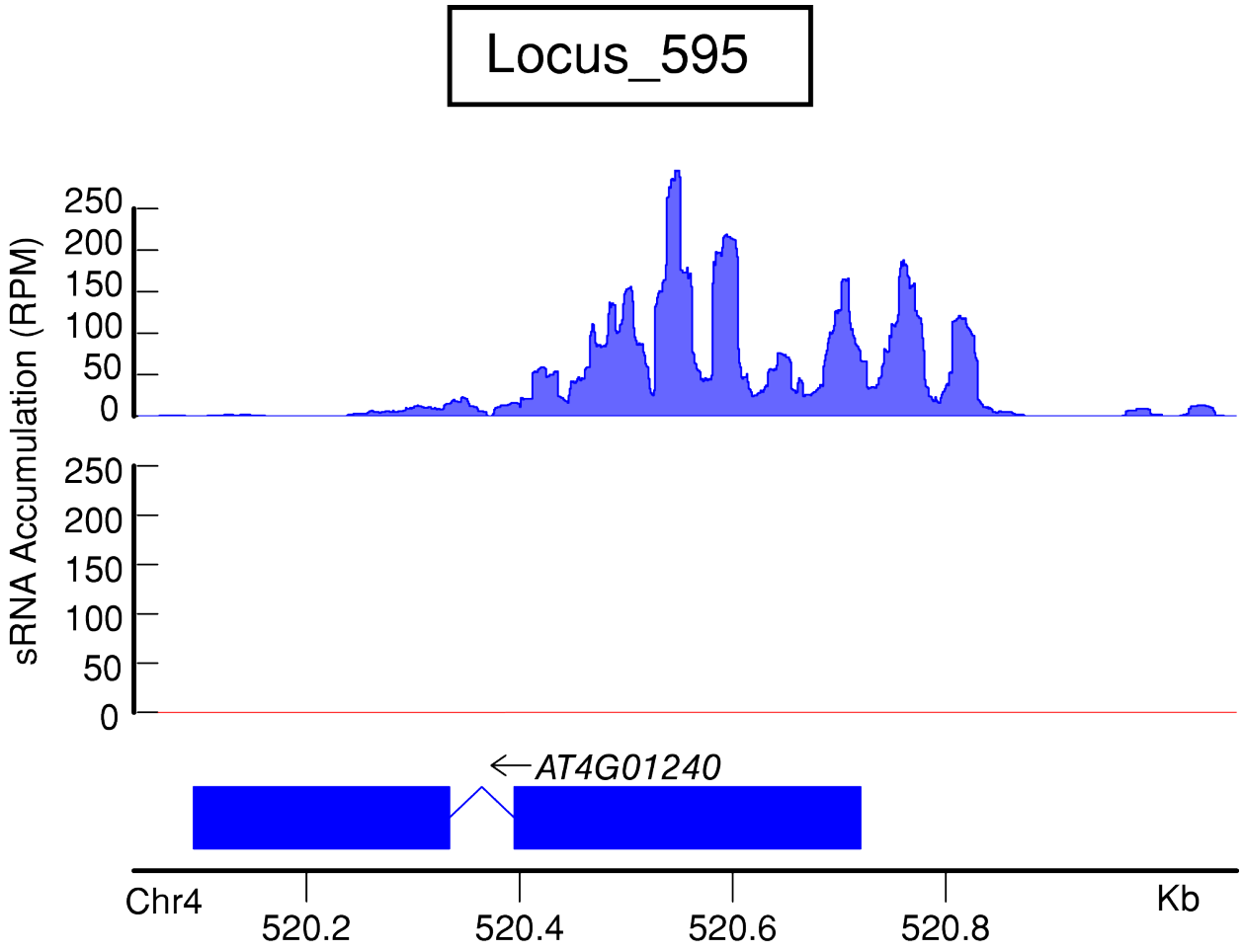

770

771

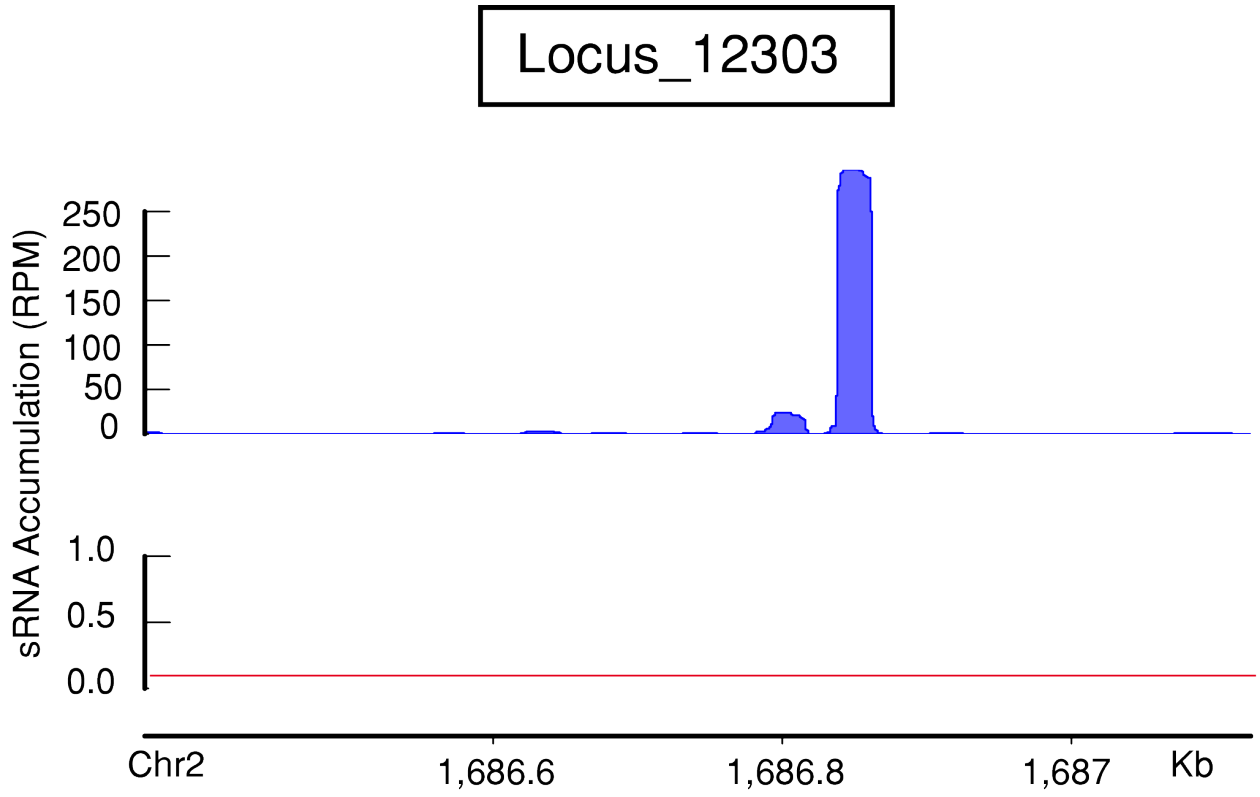

772

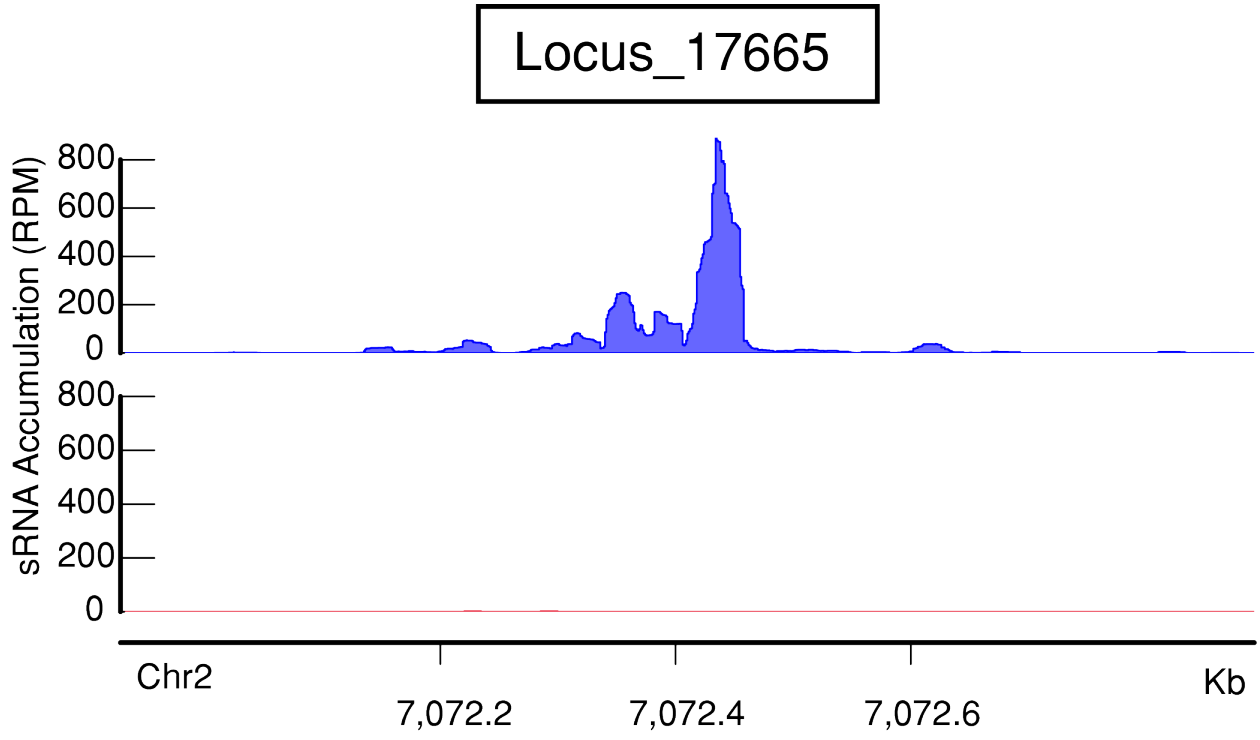

773

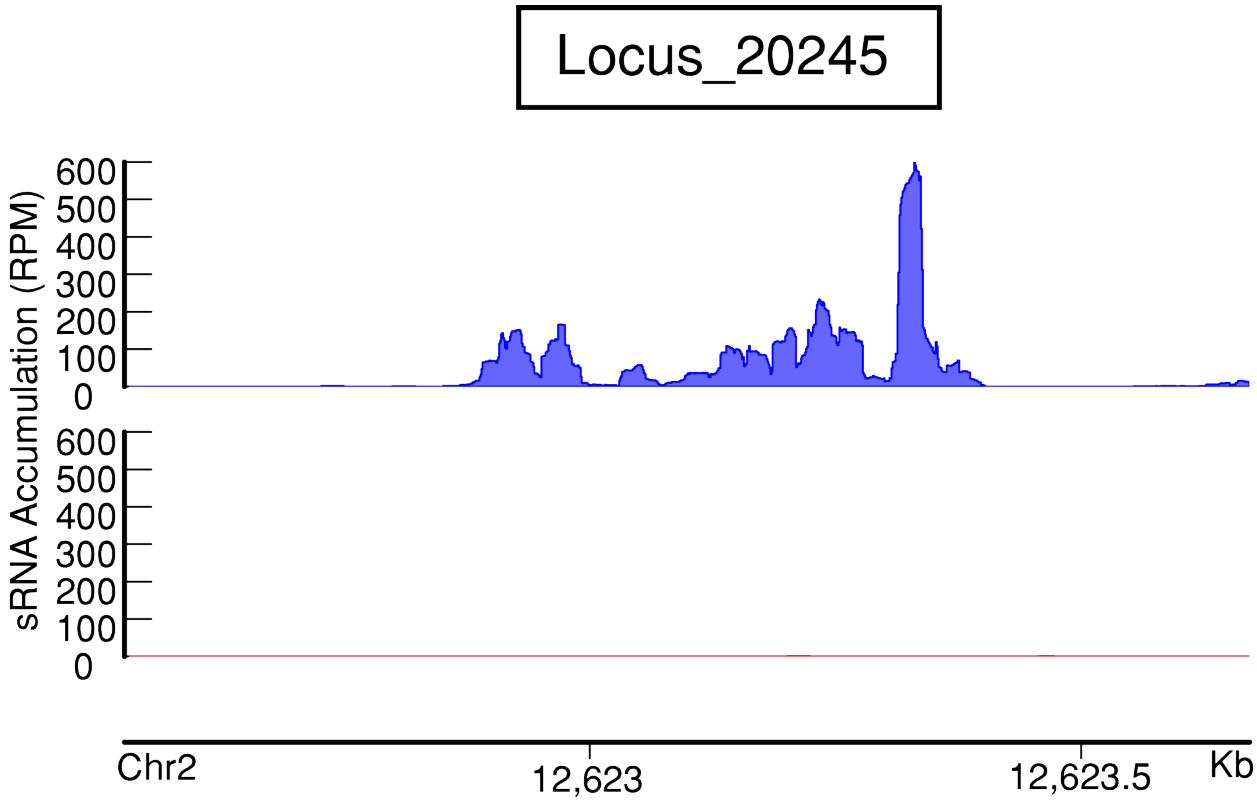

774

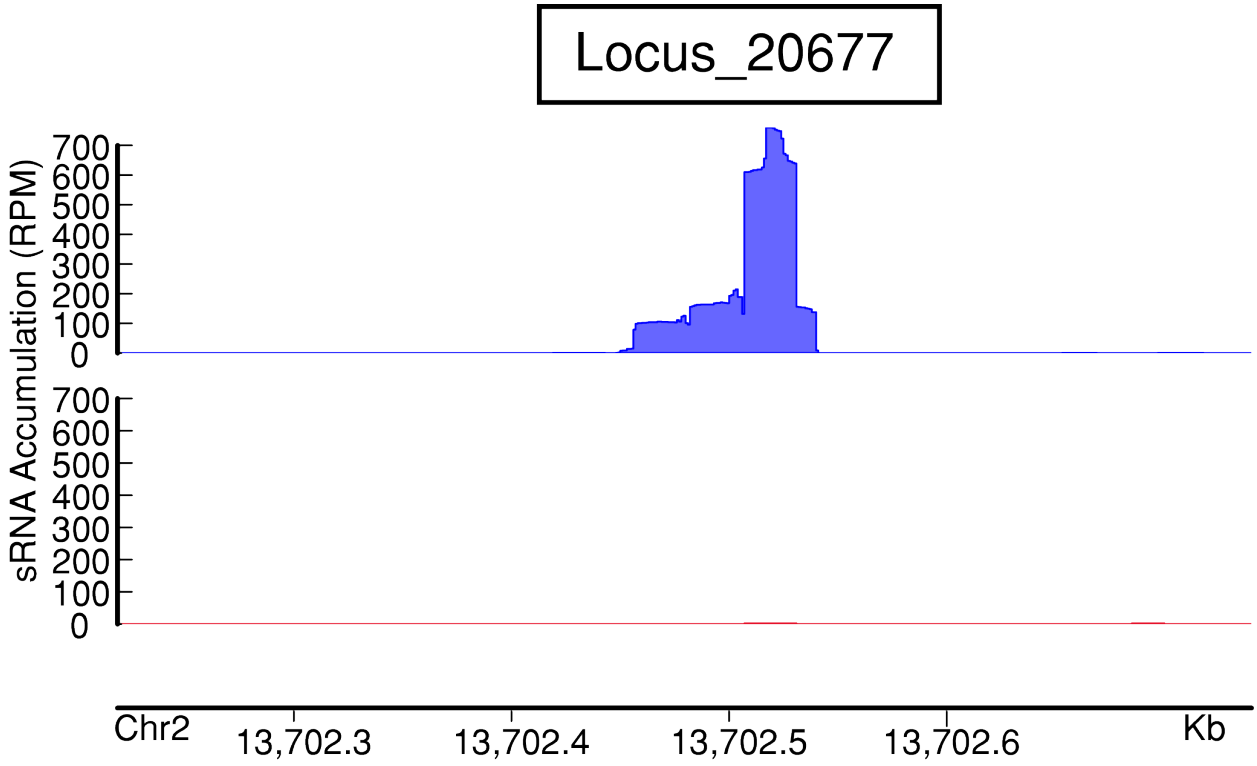

775

776

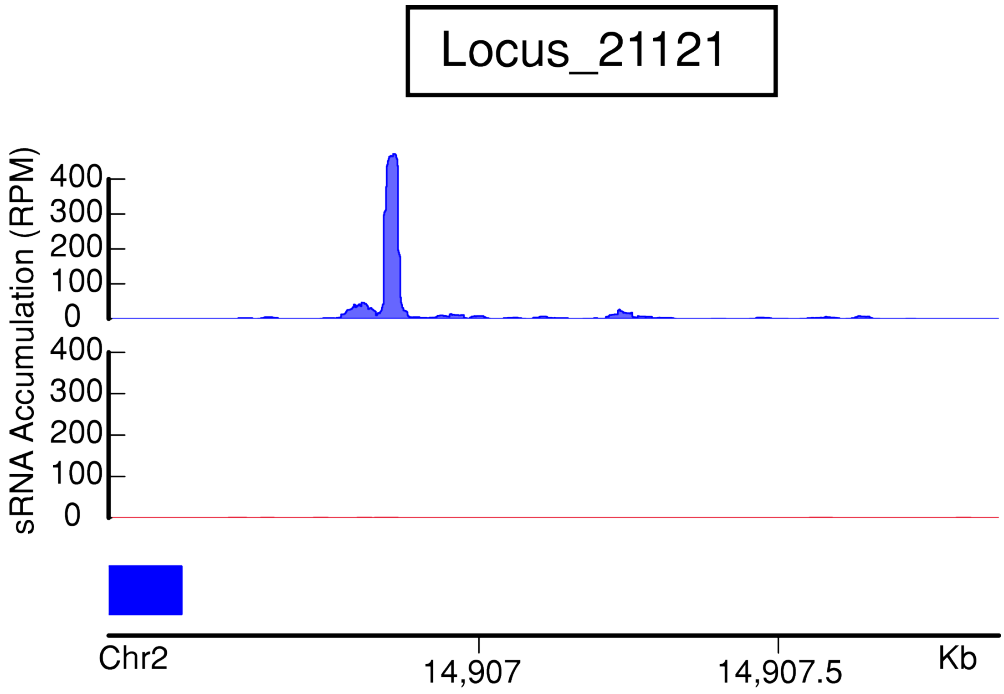

777

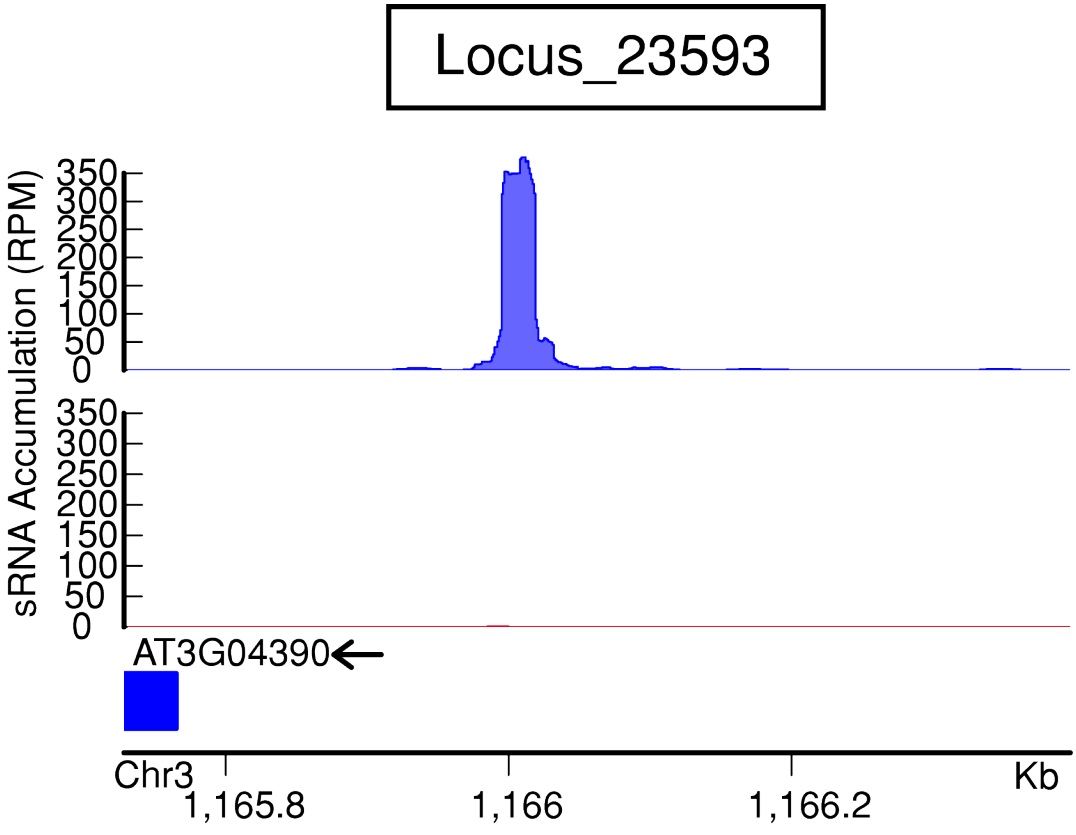

778

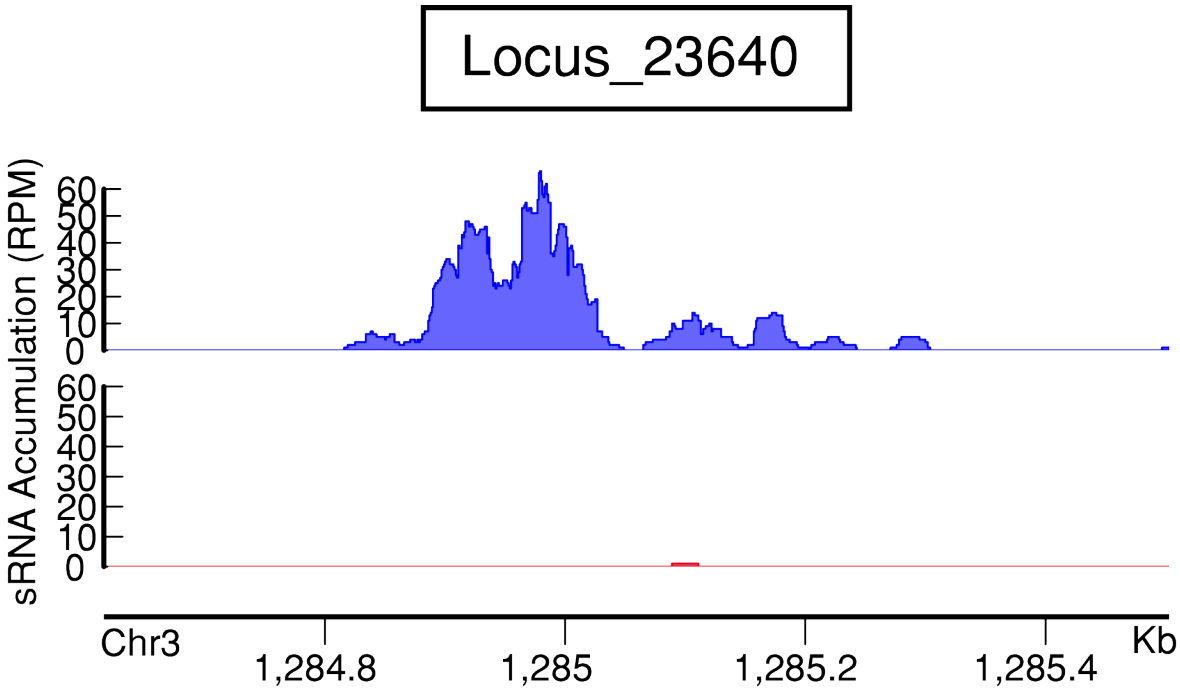

779

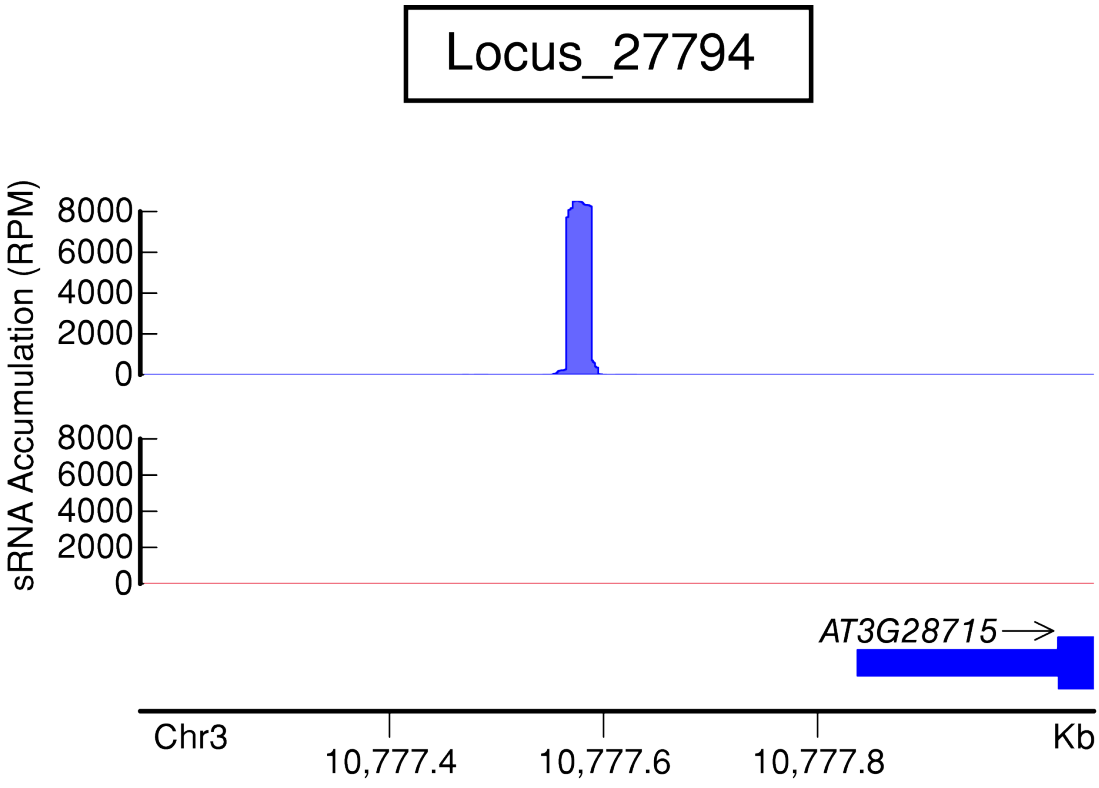

780

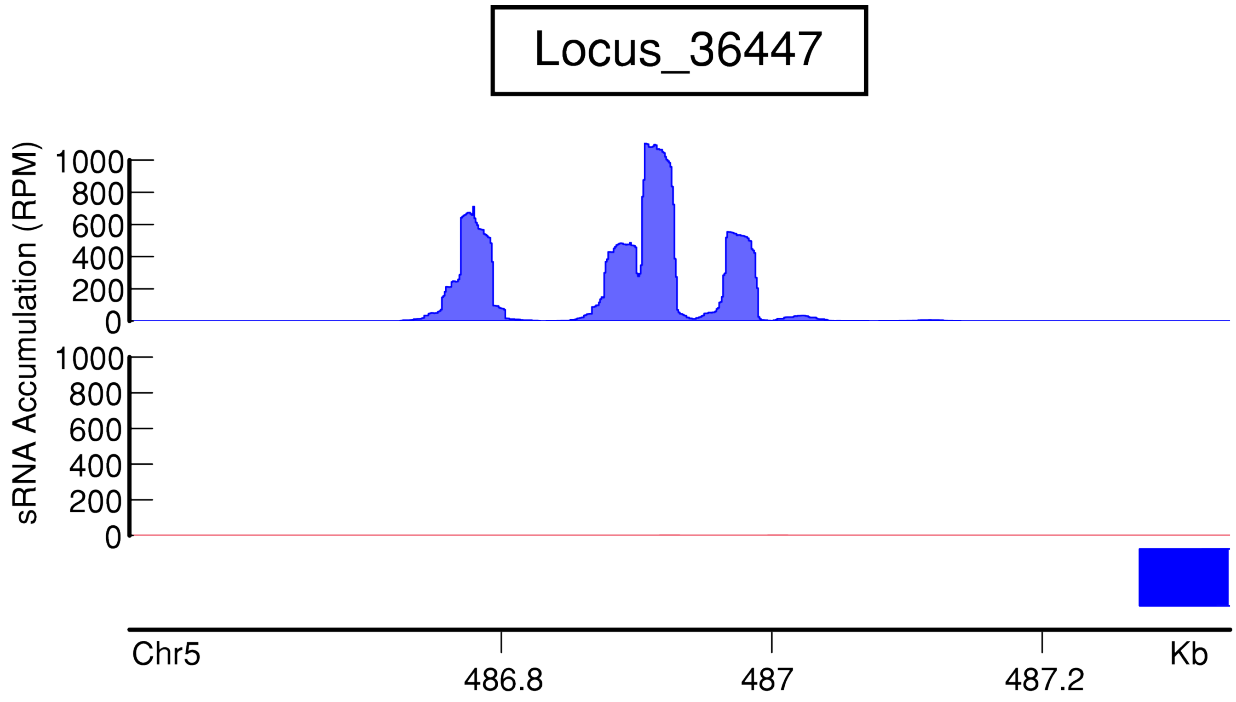

781

782

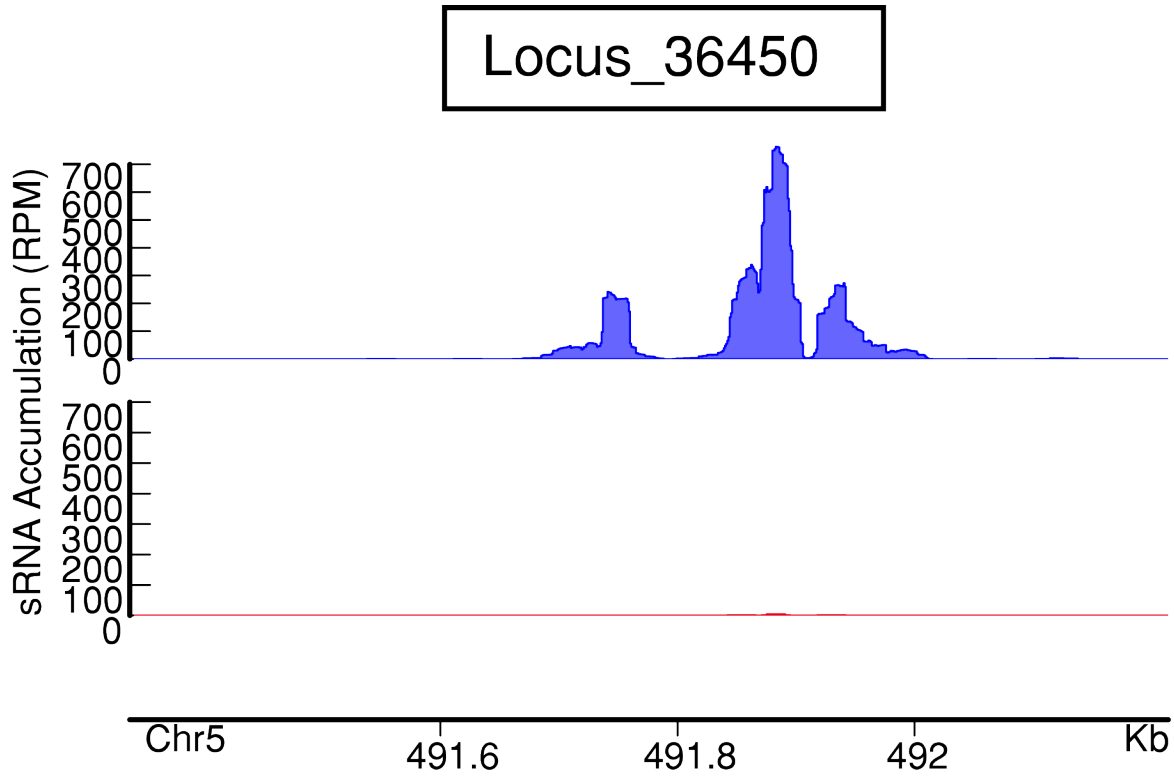

783

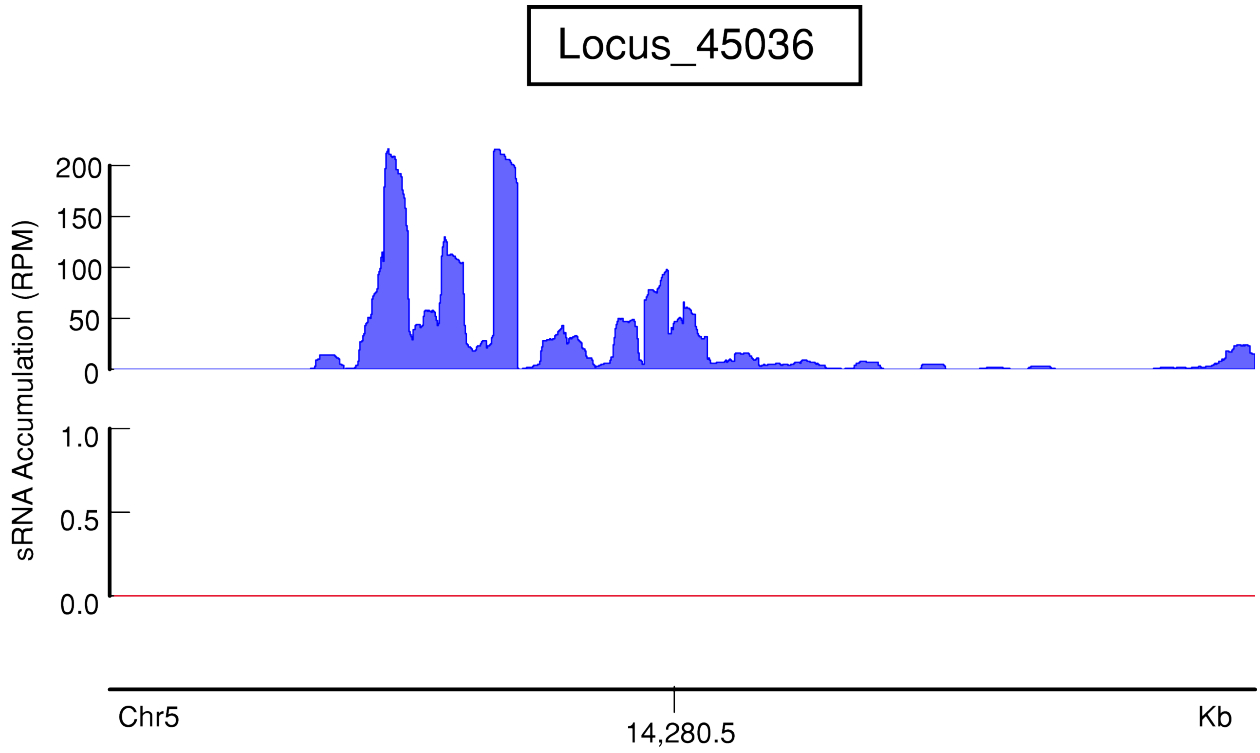

784

785

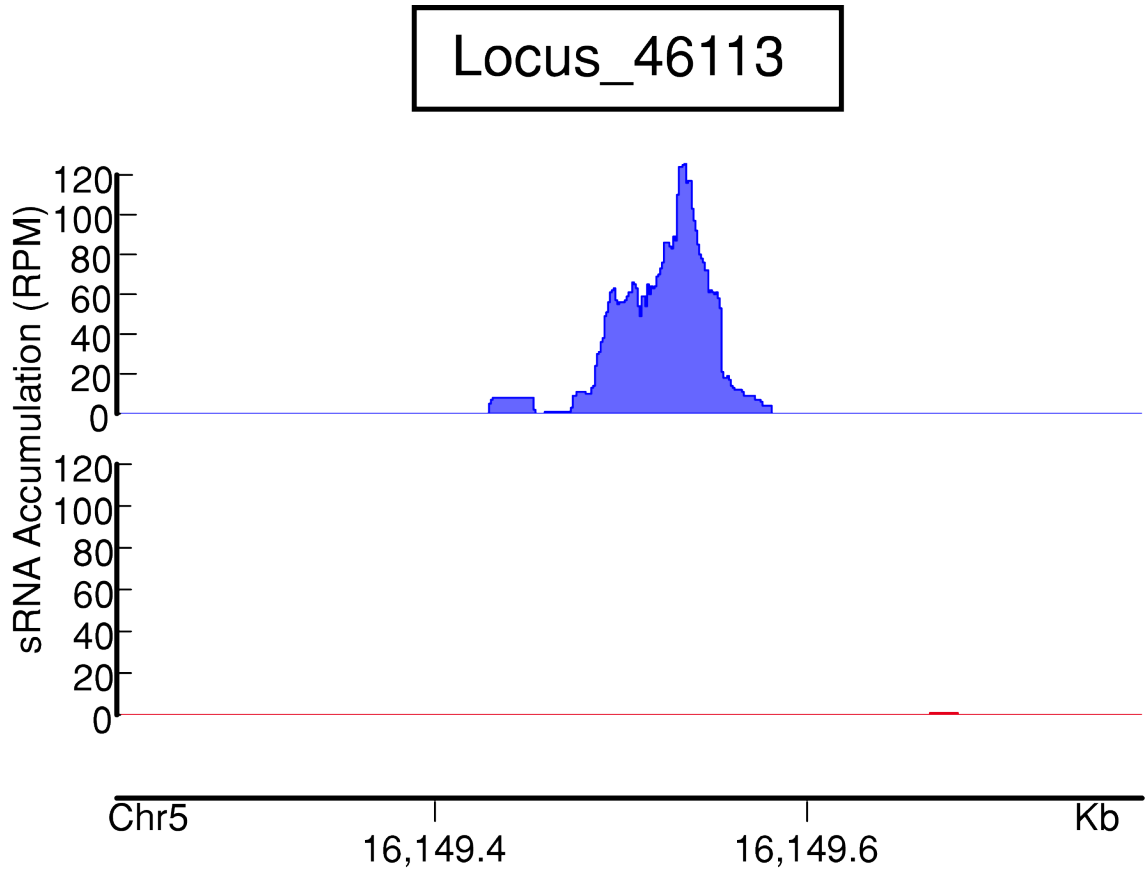

786

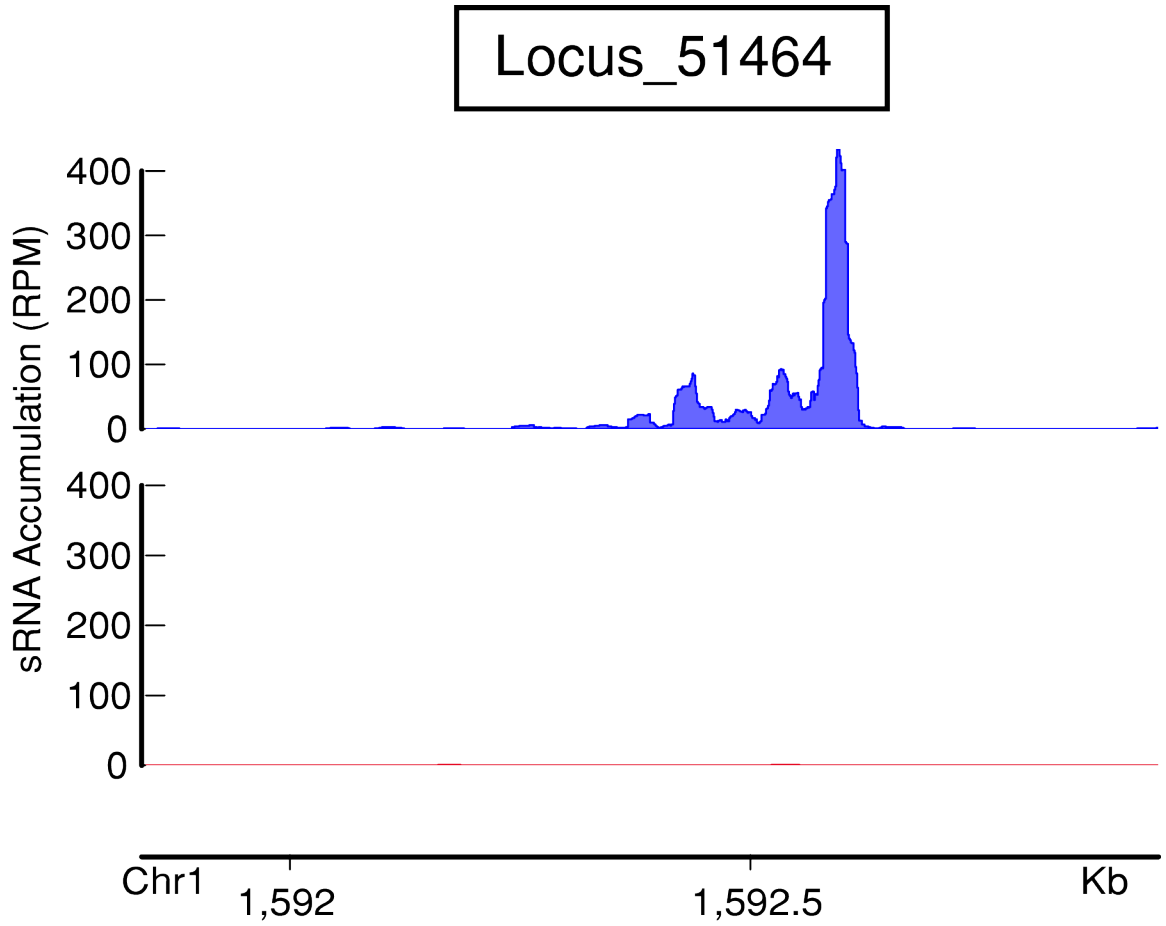

787

788

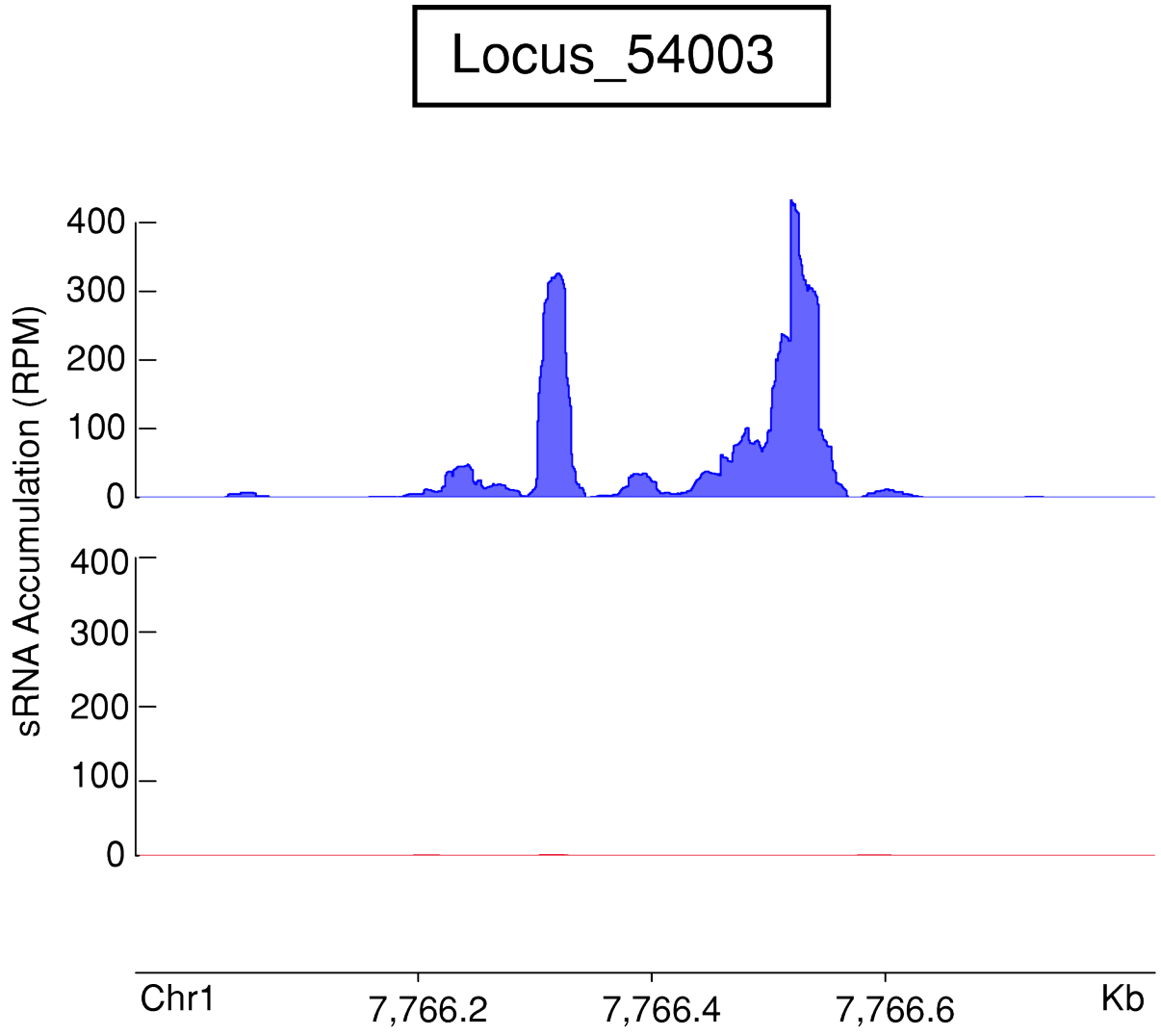

789

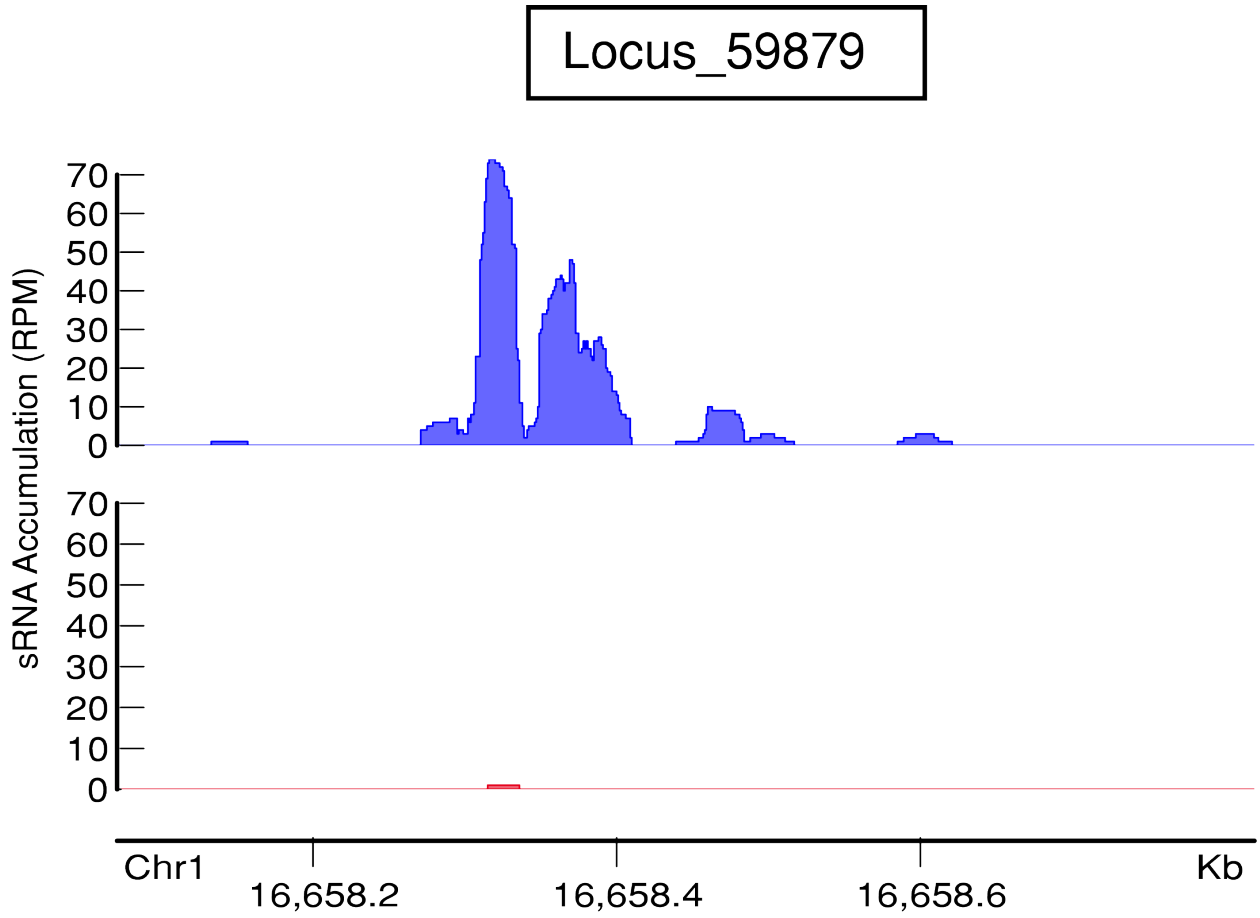

790

791

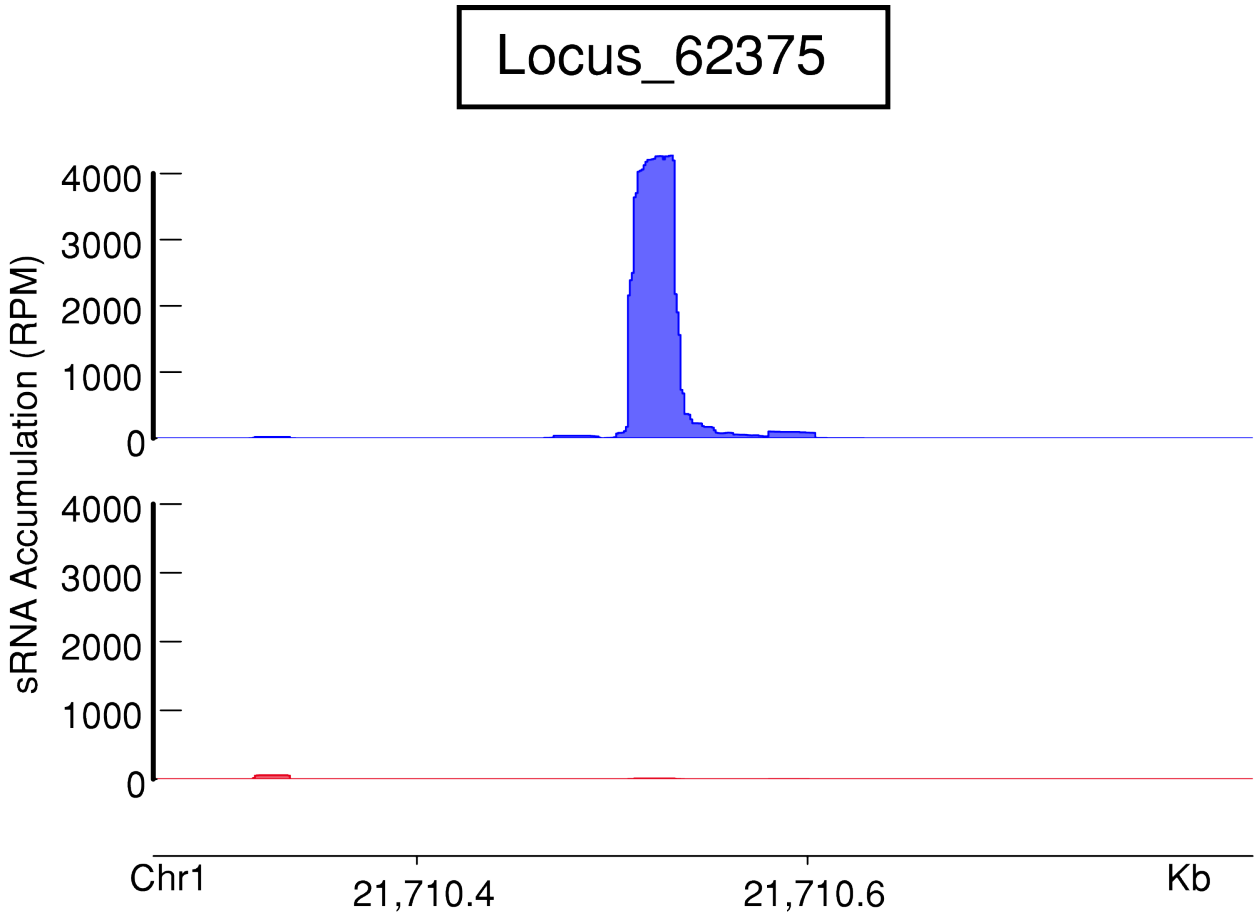

792

793

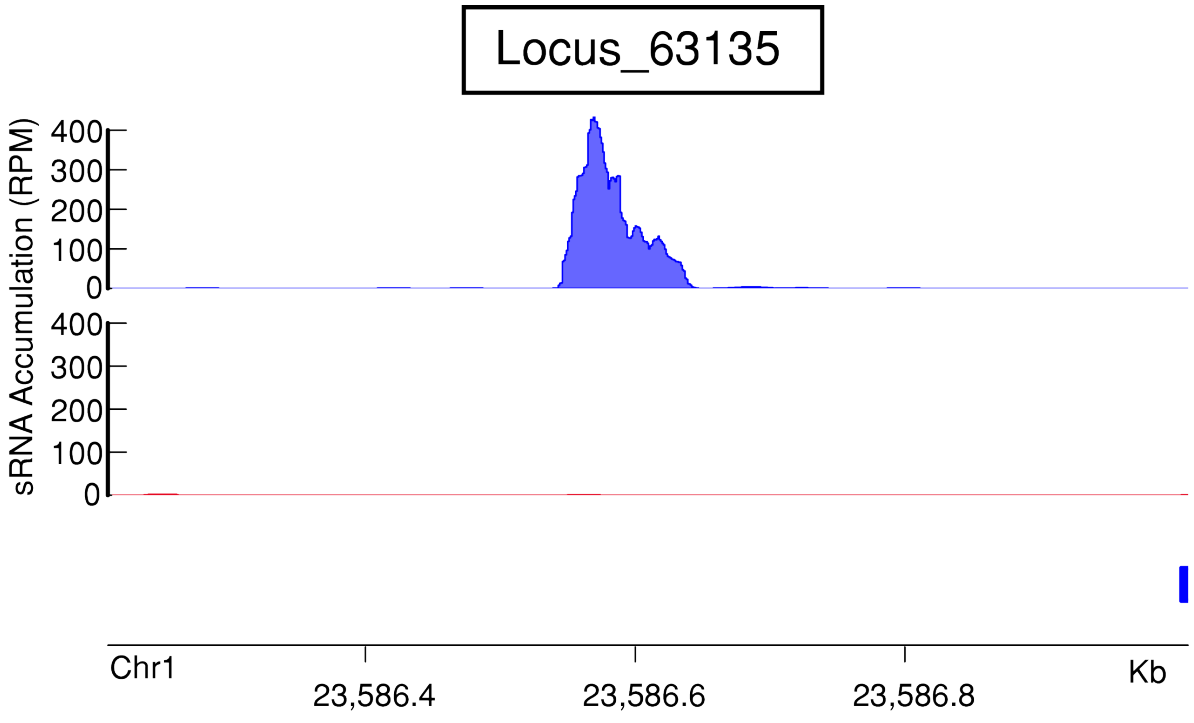

794

Figure S8. Small RNA coverage at *rdr6*-dependent, 24 nt-dominated small RNA loci.

Charts represent small RNA accumulation in RPMs at a locus (regardless of the strandedness of a read). Top chart (blue) represents accumulation in wild-type libraries, and the bottom chart (red) represents the same in *rdr1/2/6* libraries. Arrows on the gene names represent the strandedness of that gene. None had significant phasing.

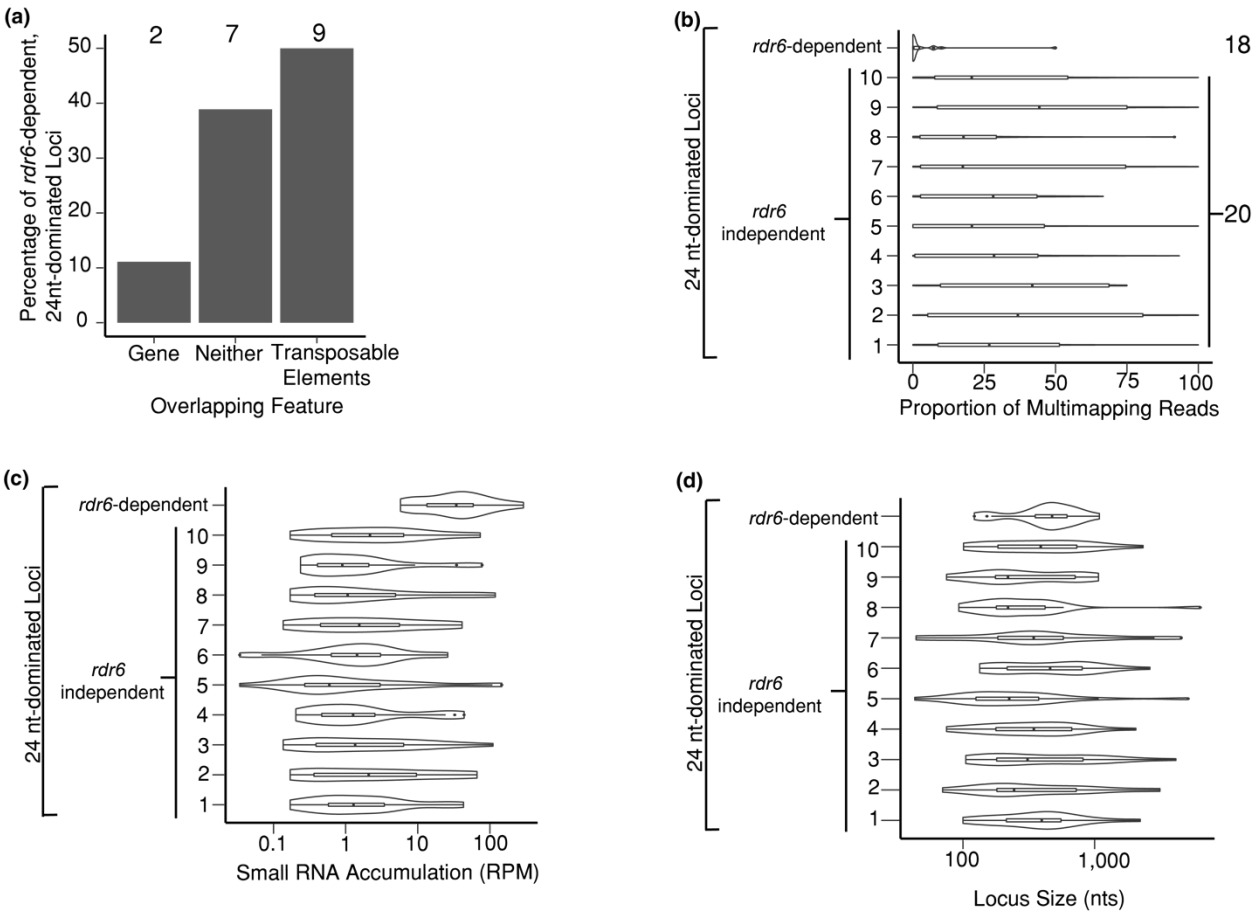

Figure S9. *rdr6*-dependent, 24 nt-dominated loci' characteristics compared to other 24nt-dominated loci.

(a) The overlap between *rdr6*-dependent, 24 nt-dominated loci with genes and transposons was calculated as in Figure 3a. Numbers at the top indicate the count in each category.

(b) The proportion of multi-mapping reads produced at *rdr6*-dependent, 24 nt-dominated loci compared to other 24 nt-dominated loci. Numbers at the top indicate the count in each category.

(c) Same as panel b except showing small RNA accumulation (in RPM). Amount in each category is the same as panel b.

(d) Same as panel b except showing length (in nts). Amount in each category is the same as panel b.

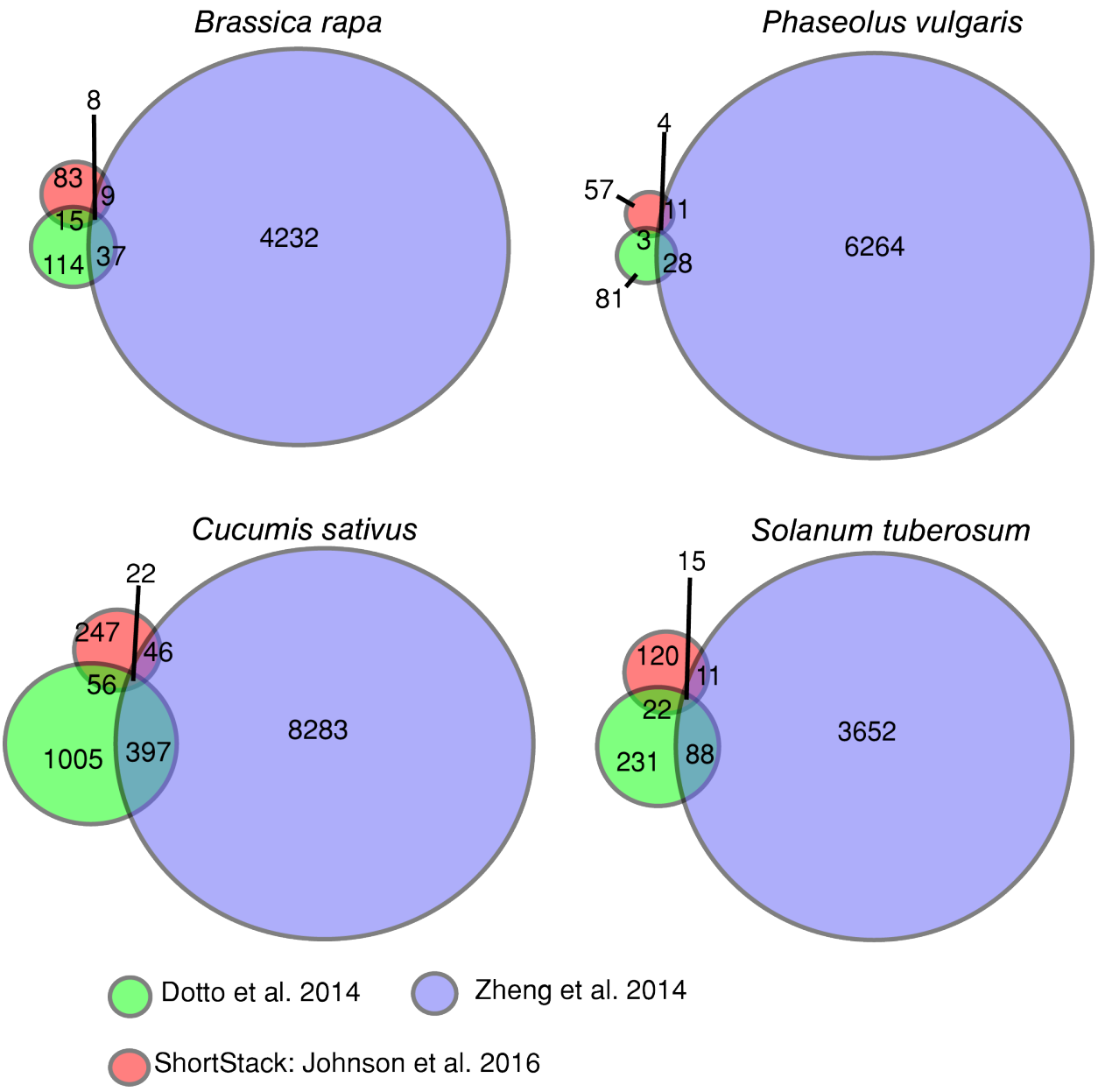

Figure S10. Several 24 nt-dominated small RNA loci pass *PHAS*-detection algorithms in four other eudicots.

Venn diagram shows numbers of 24 nt-dominated loci that were called 'phased' by the indicated algorithms. Species examined is shown above the graphs.

818 **Table S1. List of 25 known 21 nt *PHAS* loci in *A. thaliana*.**

Chr.	Start	Stop	Locus Name	Source
Chr2	11721539	11722468	*TAS1a*	(Vazquez et al., 2004)
Chr1	18549204	18550042	*TAS1b*	(Allen et al., 2005)
Chr2	16537288	16538277	*TAS1c*	(Allen et al., 2005)
Chr2	16539384	16540417	*TAS2*	(Allen et al., 2005)
Chr3	5861491	5862437	*TAS3a*	(Montgomery et al., 2008)
Chr5	20134200	20134786	*TAS3b*	(Howell et al., 2007)
Chr5	23394005	23394500	*TAS3c*	(Howell et al., 2007)
Chr3	9415004	9422587	*TAS4*	(Rajagopalan et al., 2006)
Chr1	23299057	23300958	*PPR-At1g62910*	(Ronemus et al., 2006)
Chr1	23412730	23415149	*PPR-At1g63130*	(Ronemus et al., 2006)
Chr1	23306534	23308683	*PPR-At1g62930*	(Ronemus et al., 2006)
Chr1	23387631	23390816	*PPR-At1g63080*	(Ronemus et al., 2006)
Chr1	23507320	23509053	*PPR-At1g63400*	(Ronemus et al., 2006)
Chr1	23419396	23421579	*PPR-At1g63150*	(Ronemus et al., 2006)
Chr1	23385324	23387167	*PPR-At1g63070*	(Ronemus et al., 2006)
Chr1	23489840	23491519	*PPR-At1g63330*	(Ronemus et al., 2006)
Chr1	23176930	23179248	*PPR-At1g62590*	(Ronemus et al., 2006)
Chr5	15555156	15558732	*TIR-NBS-LRR-At5g38850*	(Howell et al., 2007)
Chr1	4368760	4371293	*AFB3*	(Si-Ammour et al., 2011)
Chr5	16638370	16641728	*ATCHX18*	(Howell et al., 2007)
Chr1	17886098	17892586	*AGO1*	(Axtell et al., 2006)
Chr3	23273116	23276375	*TIR1*	(Si-Ammour et al., 2011)
Chr4	1404887	1407139	*AFB1*	(Si-Ammour et al., 2011)
Chr3	9867845	9870640	*AFB2*	(Si-Ammour et al., 2011)
Chr5	15757717	15758109	*SLG*	(Chen et al., 2007)
Chr4	8380848	8383496	*CC-NBS-LRR-At4g14610*	(Zhai et al., 2011)
Chr4	8146345	8152131	*MET2*	(Chen et al., 2010)

819

820 **Reference Cited (Table S1)**

821 **Allen, E., Xie, Z., Gustafson, A. M., & Carrington, J. C.** (2005). microRNA-directed phasing

822 during trans-acting siRNA biogenesis in plants. *Cell*, *121*(2), 207–221.

823 https://doi.org/10.1016/j.cell.2005.04.004

824 **Axtell, M. J., Jan, C., Rajagopalan, R., & Bartel, D. P.** (2006). A two-hit trigger for siRNA

825 biogenesis in plants. *Cell*, *127*(3), 565–577. https://doi.org/10.1016/j.cell.2006.09.032

826 **Chen, H.-M., Chen, L.-T., Patel, K., Li, Y.-H., Baulcombe, D. C., & Wu, S.-H.** (2010). 22-
827 nucleotide RNAs trigger secondary siRNA biogenesis in plants. *Proceedings of the*
828 *National Academy of Sciences of the United States of America*, *107*(34), 15269–15274.
829 https://doi.org/10.1073/pnas.1001738107
830 **Chen, H.-M., Li, Y.-H., & Wu, S.-H. (**2007). Bioinformatic prediction and experimental
831 validation of a microRNA-directed tandem trans-acting siRNA cascade in Arabidopsis.
832 *Proceedings of the National Academy of Sciences*, *104*(9), 3318–3323.
833 https://doi.org/10.1073/pnas.0611119104
834 **Howell, M. D., Fahlgren, N., Chapman, E. J., Cumbie, J. S., Sullivan, C. M., Givan, S. A.,**
835 **& Carrington, J. C.** (2007). Genome-Wide Analysis of the RNA-DEPENDENT RNA
836 POLYMERASE6/DICER-LIKE4 Pathway in Arabidopsis Reveals Dependency on
837 miRNA- and tasiRNA-Directed Targeting. *The Plant Cell*, *19*(3), 926–942.
838 https://doi.org/10.1105/tpc.107.050062
839 **Montgomery, T. A., Howell, M. D., Cuperus, J. T., Li, D., Hansen, J. E., Alexander, A. L.,**
840 **& Carrington, J. C.** (2008). Specificity of ARGONAUTE7-miR390 Interaction and
841 Dual Functionality in TAS3 Trans-Acting siRNA Formation. *Cell*, *133*(1), 128–141.
842 https://doi.org/10.1016/j.cell.2008.02.033
843 **Rajagopalan, R., Vaucheret, H., Trejo, J., & Bartel, D. P.** (2006). A diverse and
844 evolutionarily fluid set of microRNAs in Arabidopsis thaliana. *Genes & Development*,
845 *20*(24), 3407–3425. https://doi.org/10.1101/gad.1476406
846 **Ronemus, M., Vaughn, M. W., & Martienssen, R. A**. (2006). MicroRNA-Targeted and Small
847 Interfering RNA–Mediated mRNA Degradation Is Regulated by Argonaute, Dicer, and

RNA-Dependent RNA Polymerase in Arabidopsis. *The Plant Cell*, *18*(7), 1559–1574. https://doi.org/10.1105/tpc.106.042127

Si-Ammour, A., Windels, D., Arn-Bouldoires, E., Kutter, C., Ailhas, J., Meins, F., & Vazquez, F. (2011). miR393 and Secondary siRNAs Regulate Expression of the TIR1/AFB2 Auxin Receptor Clade and Auxin-Related Development of Arabidopsis Leaves. *Plant Physiology*, *157*(2), 683–691. https://doi.org/10.1104/pp.111.180083

Vazquez, F., Vaucheret, H., Rajagopalan, R., Lepers, C., Gasciolli, V., Mallory, A. C., & Crété, P. (2004). Endogenous trans-Acting siRNAs Regulate the Accumulation of Arabidopsis mRNAs. *Molecular Cell*, *16*(1), 69–79. https://doi.org/10.1016/j.molcel.2004.09.028

Zhai, J., Jeong, D.-H., Paoli, E. D., Park, S., Rosen, B. D., Li, Y., & Meyers, B. C. (2011). MicroRNAs as master regulators of the plant NB-LRR defense gene family via the production of phased, trans-acting siRNAs. *Genes & Development*, *25*(23), 2540–2553. https://doi.org/10.1101/gad.177527.111

874 **Table S2. *A. thaliana* small RNA libraries used in this study**

Accession Number	Genotype	3' Adapter (First 8 nts)	Source
GSM2825283	Wild-type Replicate 1	TGGAATTC	(Polydore & Axtell, 2018)
GSM2825284	Wild-type Replicate 2	TGGAATTC	(Polydore & Axtell, 2018)
GSM2825285	Wild-type Replicate 3	TGGAATTC	(Polydore & Axtell, 2018)
GSM2825286	*rdr1-1/2-1/6-15* Replicate 1	TGGAATTC	(Polydore & Axtell, 2018)
GSM2825287	*rdr1-1/2-1/6-15* Replicate 2	TGGAATTC	(Polydore & Axtell, 2018)
GSM2825288	*rdr1-1/2-1/6-15* Replicate 3	TGGAATTC	(Polydore & Axtell, 2018)
GSM1533527	Wild-type Replicate 1	TGGAATTC	(Groth et al., 2014)
GSM1533528	Wild-type Replicate 2	TGGAATTC	(Groth et al., 2014)
GSM1533529	Wild-type Replicate 3	TGGAATTC	(Groth et al., 2014)
GSM1533542	*dcl3* Replicate 1	TGGAATTC	(Groth et al., 2014)
GSM1533543	*dcl3* Replicate 2	TGGAATTC	(Groth et al., 2014)
GSM1533544	*dcl3* Replicate 3	TGGAATTC	(Groth et al., 2014)
GSM1845210	Wild-type Replicate 1	AGATCGGA	(Elvira-Matelot et al., 2016)
GSM1845211	Wild-type Replicate 2	AGATCGGA	(Elvira-Matelot et al., 2016)
GSM1845212	Wild-type Replicate 3	AGATCGGA	(Elvira-Matelot et al., 2016)
GSM1845222	*dcl2-1/3-1/4-2t* Replicate 1	AGATCGGA	(Elvira-Matelot et al., 2016)
GSM1845223	*dcl2-1/3-1/4-2t* Replicate 2	AGATCGGA	(Elvira-Matelot et al., 2016)
GSM1845224	*dcl2-1/3-1/4-2t* Replicate 3	AGATCGGA	(Elvira-Matelot et al., 2016)
GSM1087973	Wild-type Replicate 1	TCGTATGC	(Jeong et al., 2013)
GSM1087974	Wild-type Replicate 2	TCGTATGC	(Jeong et al., 2013)
GSM1087975	*dcl1-7* Replicate 1	TCGTATGC	(Jeong et al., 2013)
GSM1087976	*dcl1-7* Replicate 2	TCGTATGC	(Jeong et al., 2013)
GSM1377370	Wild-type Replicate 1	TGGAATTC	(Li et al., 2014)
GSM1377371	Wild-type Replicate 2	TGGAATTC	(Li et al., 2014)
GSM1377372	*nrpd1-3* Replicate 1	TGGAATTC	(Li et al., 2014)
GSM1377373	*nrpd1-3* Replicate 2	TGGAATTC	(Li et al., 2014)
GSM1377376	*rdr2-1* Replicate 1	TGGAATTC	(Li et al., 2014)

GSM1377377	*rdr2-1* Replicate 2	TGGAATTC	(Li et al., 2014)
GSM2102962	Wild-type Replicate 1	TGGAATTC	(Panda et al., 2016)
GSM2102963	Wild-type Replicate 2	TGGAATTC	(Panda et al., 2016)
GSM2102965	*rdr6-15* Replicate 1	TGGAATTC	(Panda et al., 2016)
GSM2102462	*rdr6-15* Replicate 2	TGGAATTC	(Panda et al., 2016)
GSM893112	Wild-type Replicate 1	CACTCGGG	(Lee et al., 2012)
GSM893113	Wild-type Replicate 2	CACTCGGG	(Lee et al., 2012)
GSM893114	Wild-type Replicate 3	CACTCGGG	(Lee et al., 2012)
GSM893115	*nrpb1-1 (nrpe)* Replicate 1	CACTCGGG	(Lee et al., 2012)
GSM893116	*nrpb1-1 (nrpe)* Replicate 2	CACTCGGG	(Lee et al., 2012)
GSM893117	*nrpb1-1 (nrpe)* Replicate 3	CACTCGGG	(Lee et al., 2012)
GSM1668899	Wild-type Replicate 1	TGGAATTC	(Zhai et al., 2015)
GSM1668905	Wild-type Replicate 2	TGGAATTC	(Zhai et al., 2015)

Reference List (Table S2)

Elvira-Matelot, E., Hachet, M., Shamandi, N., Comella, P., Sáez-Vásquez, J., Zytnicki, M., & Vaucheret, H. (2016). Arabidopsis RNASE THREE LIKE2 Modulates the Expression of Protein-Coding Genes via 24-Nucleotide Small Interfering RNA-Directed DNA Methylation. *The Plant Cell Online*, *28*(2), 406–425. https://doi.org/10.1105/tpc.15.00540

Groth, M., Stroud, H., Feng, S., Greenberg, M. V. C., Vashisht, A. A., Wohlschlegel, J. A., & Ausin, I. (2014). SNF2 chromatin remodeler-family proteins FRG1 and -2 are required for RNA-directed DNA methylation. *Proceedings of the National Academy of Sciences of the United States of America*, *111*(49), 17666–17671. https://doi.org/10.1073/pnas.1420515111

Jeong, D.-H., Thatcher, S. R., Brown, R. S. H., Zhai, J., Park, S., Rymarquis, L. A., & Green, P. J. (2013). Comprehensive Investigation of MicroRNAs Enhanced by Analysis of Sequence Variants, Expression Patterns, ARGONAUTE Loading, and Target Cleavage1[W][OA]. *Plant Physiology*, *162*(3), 1225–1245. https://doi.org/10.1104/pp.113.219873

Lee, T., Gurazada, S. G. R., Zhai, J., Li, S., Simon, S. A., Matzke, M. A., & Meyers, B. C. (2012). RNA polymerase V-dependent small RNAs in Arabidopsis originate from small, intergenic loci including most SINE repeats. *Epigenetics*, *7*(7), 781–795. https://doi.org/10.4161/epi.20290

Li, S., Vandivier, L. E., Tu, B., Gao, L., Won, S. Y., Li, S., & Chen, X. (2014). Detection of Pol IV/RDR2-dependent transcripts at the genomic scale in Arabidopsis reveals features and regulation of siRNA biogenesis. *Genome Research*, gr.182238.114. https://doi.org/10.1101/gr.182238.114

Panda, K., Ji, L., Neumann, D. A., Daron, J., Schmitz, R. J., & Slotkin, R. K. (2016). Full-length autonomous transposable elements are preferentially targeted by expression-dependent forms of RNA-directed DNA methylation. *Genome Biology*, *17*, 170. https://doi.org/10.1186/s13059-016-1032-y

Polydore, S., & Axtell, M. J. (2018). Analysis of RDR1/RDR2/RDR6-independent small RNAs in Arabidopsis thaliana improves MIRNA annotations and reveals unexplained types of short interfering RNA loci. *The Plant Journal: For Cell and Molecular Biology*, *94*(6), 1051–1063. https://doi.org/10.1111/tpj.13919

Zhai, J., Bischof, S., Wang, H., Feng, S., Lee, T., Teng, C., & Jacobsen, S. E. (2015). One precursor One siRNA model for Pol IV- dependent siRNAs Biogenesis. *Cell*, *163*(2), 445–455. https://doi.org/10.1016/j.cell.2015.09.032